the development of cardiac hypertrophy (Seth *et al*, 2004). Other groups reported that TRPM7 regulates Mg^{2+} homeostasis, and TRPM6 and TRPM7 are differentially regulated by Ang II in vascular smooth muscle cells (He *et al*, 2005; Touyz *et al*, 2006). However, it is still unknown whether TRP channels contribute to receptor-stimulated activation of calcineurin-NFAT pathway in the heart. In this study, we investigated the mechanism of how Ang II stimulation induces the sustained Ca^{2+} signaling leading to NFAT activation and hypertrophic growth of rat neonatal cardiomyocytes.

Results

Essential role of DAG in Ang II-induced NFAT activation and cardiac hypertrophy

We first examined whether IP_3 or DAG is involved in Ang II-induced NFAT activation in rat neonatal cardiomyocytes. As it has been reported that pressure overload- and Ang II-induced cardiac hypertrophy are attenuated in NFAT4 (NFATc3)-null mice (Wilkins *et al*, 2002), the translocation of NFAT4 was determined in this study. Stimulation of cardiac myocytes with Ang II for 30 min increased the maximal nuclear predominant fluorescence of GFP-fused amino-terminal region of NFAT4 protein (GFP-NFAT4) (Figure 1A–C). The Ang II-induced NFAT translocation was completely suppressed by the expression of DAG kinase β (DGKβ), an enzyme that decreases the cellular DAG level by converting DAG to phosphatidic acid. Treatment with RHC80267, a DAG lipase inhibitor, significantly increased the Ang II-induced nuclear translocation of GFP-NFAT4. However, treatment with xestospongin C, an IP_3R blocker, did not affect the Ang II-induced translocation of GFP-NFAT4 to the nucleus. To directly inhibit IP_3-mediated signaling, we expressed the ligand-binding region of type 1 IP_3R (IP_3-sponge) (Uchiyama *et al*, 2002).

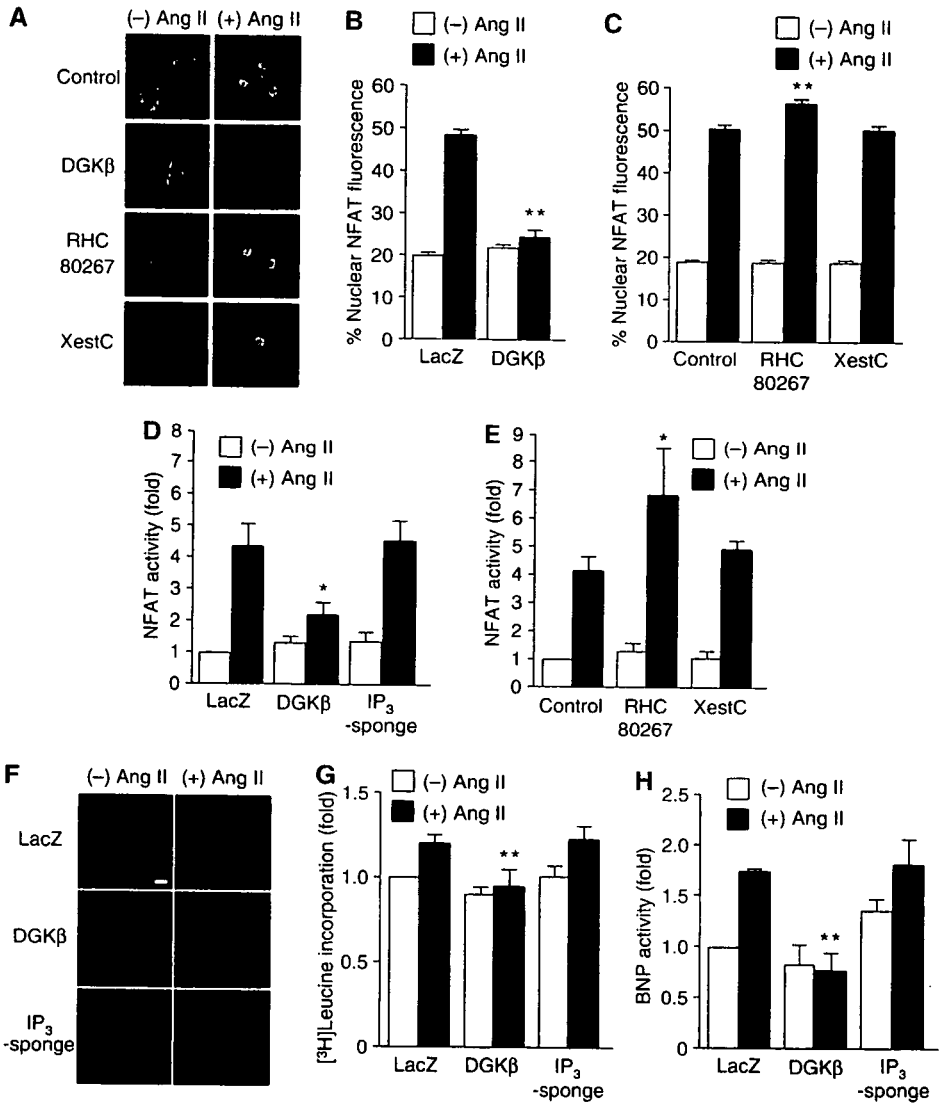

Figure 1 Essential role of DAG in Ang II-induced cardiomyocyte hypertrophy. (**A**) Nuclear translocation of GFP-NFAT4 by Ang II stimulation. A portion of cells was treated with RHC80267 (30 μM) or xestospongin C (XestC, 20 μM) for 30 min before the addition of Ang II (100 nM), and a portion of cells was infected with DGKβ for 48 h before Ang II stimulation. (**B**, **C**) Quantification of nuclear predominant fluorescence of GFP-NFAT4 after Ang II stimulation. (**D**, **E**) Effects of DGKβ, RHC80267, and XestC on the increase in NFAT-dependent luciferase activity by Ang II stimulation for 6 h. The fold activation was calculated by the values of untreated cells set as 1. (**F**–**H**) Effects of DGKβ and GFP-IP_3-sponge on Ang II-induced actin reorganization (**F**), protein synthesis (**G**), and BNP expression (**H**). Scale bar = 20 μm. $^*P<0.05$, $^{**}P<0.01$ versus control or LacZ-expressing cells.

The Ang II-induced transient increase in $[Ca^{2+}]_i$ (or Ca^{2+} release) was completely suppressed by the treatment with xestospongin C and by the expression of IP_3-sponge but not DGKβ (Supplementary Figure S1), suggesting the efficient inhibition of IP_3-mediated Ca^{2+} signaling. The Ang II-induced increase in NFAT-dependent luciferase reporter activity was suppressed by DGKβ, but not by xestospongin C and IP_3-sponge (Figure 1D and E). Treatment with RHC80267 promoted the Ang II-induced NFAT activation (Figure 1E). These results suggest the involvement of DAG in Ang II-induced NFAT activation. We also examined the involvement of DAG in Ang II-induced hypertrophic responses. Expression of DGKβ, but not IP_3-sponge, completely suppressed Ang II-induced hypertrophic responses, such as actin reorganization (Figure 1F), protein synthesis (Figure 1G), and expression of brain natriuretic peptide (BNP) (Figure 1H). These results suggest that DAG, but not IP_3, is essential for Ang II-induced NFAT activation and hypertrophic responses of neonatal cardiomyocytes.

Involvement of Ang II type 1 receptor, $G\alpha_q$, and PLC in Ang II-induced NFAT activation

In contrast to the absence of extracellular Ca^{2+} (Supplementary Figure S1A), myocytes showed spontaneous increases in $[Ca^{2+}]_i$ in the presence of extracellular Ca^{2+}. Treatment with Ang II induced the transient increase in $[Ca^{2+}]_i$ followed by sustained oscillatory increase in $[Ca^{2+}]_i$ (Figure 2A; the former can more clearly be seen in Supplementary Figure S1A). The Ca^{2+} oscillation represents a spontaneous activity of myocytes, and Ang II stimulation increased its frequency (Supplementary Figure S1C). The Ang II-induced Ca^{2+} response and NFAT activation were greatly suppressed by U73122, a PLC inhibitor, but not by U73343, an inactive analog of U73122 (Figure 2A–C). Thus, PLC primarily regulates Ang II-induced Ca^{2+} signal generation. The Ang II-induced translocation of GFP-NFAT4 was suppressed by CV11974, an Ang II type 1 receptor (AT1R) blocker, but not by PD123319, an AT2R blocker (Figure 2D). These results indicate that AT1R-mediated PLC activation is

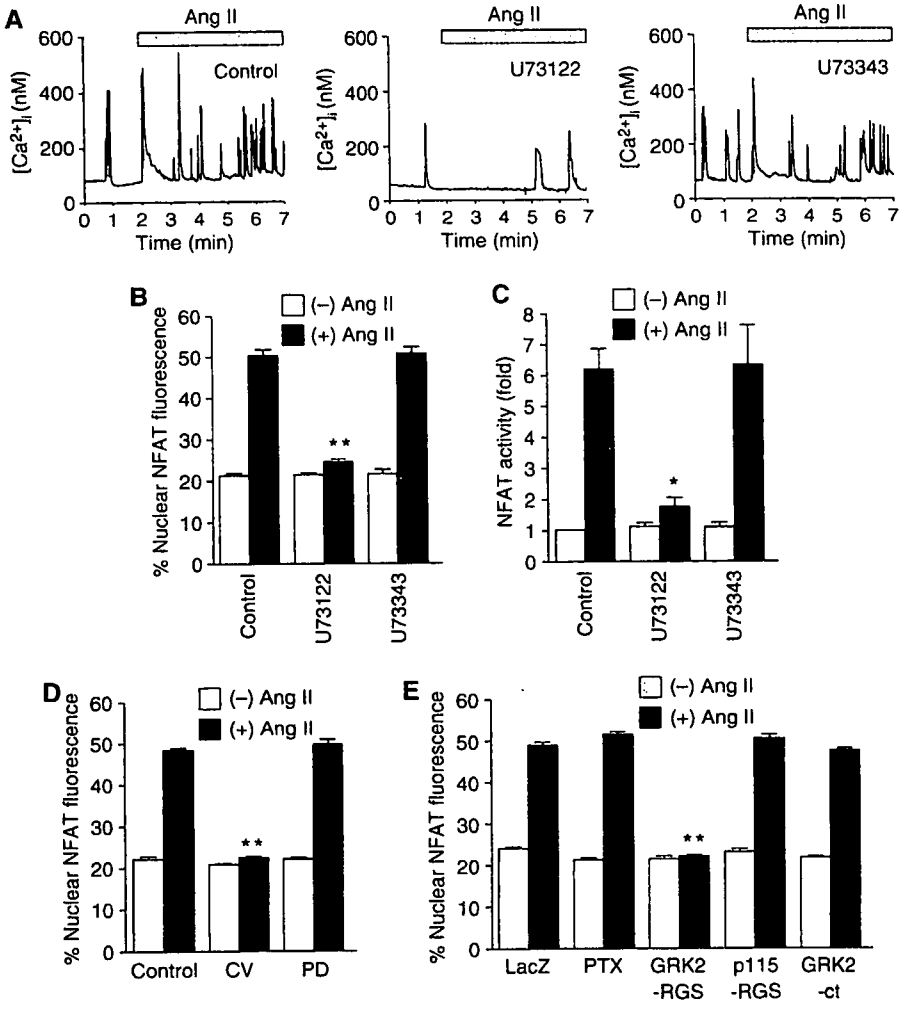

Figure 2 Involvement of AT1R, $G\alpha_q$, and PLC in Ang II-induced NFAT activation. (**A–C**) Effects of U73122 and U73343 on Ang II-induced Ca^{2+} responses (**A**), translocation of GFP-NFAT4 (**B**), and NFAT activation (**C**). (A) Effects of U73122 and U73343 on the increases in the frequency of Ca^{2+} oscillation during 5 min Ang II stimulation. The digital images were obtained every 1 s. (**D**) Effects of CV11974 and PD123319 on Ang II-induced NFAT translocation. Cells were treated with U73122 (5 μM), U73343 (5 μM), CV11974 (CV, 5 μM), or PD123319 (PD, 5 μM) for 30 min before the addition of Ang II (100 nM). (**E**) Effects of PTX, GRK2-RGS, p115-RGS, and GRK2-ct on Ang II-induced NFAT translocation. Cells were infected with adenovirus encoding LacZ (100 MOI), p115-RGS or GRK2-ct (100 MOI), or GRK2-RGS (300 MOI) for 48 h. A portion of cells was treated with PTX (100 ng/ml) for 24 h before Ang II stimulation. $^*P<0.05$, $^{**}P<0.01$ versus Ang II stimulation of control or LacZ-expressing cells.

involved in Ang II-induced NFAT4 activation. We next examined which G proteins are involved in Ang II-induced NFAT activation. It has been generally believed that $G\alpha_q$ plays an important role in agonist-induced cardiac hypertrophy (Molkentin and Dorn, 2001). To examine the involvement of $G\alpha_q$, we expressed regulator of G protein signaling (RGS) domain that is ~200 amino acids, specifically binds GTP-bound form of Gα and accelerates GTPase activity. When RGS domain is expressed in cells, it competes with activated form of Gα for endogenous effectors and accelerates turn-off reaction of Gα. Therefore, RGS domain can work as a specific inhibitor of Gα. As expected, the expression of a $G\alpha_q$-specific RGS domain of G protein-coupled receptor kinase 2 (GRK2-RGS) completely suppressed the Ang II-induced translocation of GFP-NFAT4 (Figure 2E). However, the expression of a $G\alpha_{12/13}$-specific RGS domain of p115RhoGEF (p115-RGS) did not affect the Ang II-induced translocation of GFP-NFAT4. *Pertussis* toxin (PTX) and carboxyl terminal region of GRK2 (GRK2-ct), a βγ subunit of G protein (Gβγ)-sequestering polypeptide, did not inhibit the Ang II-induced translocation of GFP-NFAT4 (Figure 2E). Thus, these results support the evidence that agonist-induced Ca^{2+}-dependent NFAT activation is predominantly regulated by $G\alpha_q$, but not by $G\alpha_{12/13}$, G_i or Gβγ in cardiomyocytes.

Requirement of Ca^{2+} influx through L-type Ca^{2+} channels and nonselective cation channels in Ang II-induced NFAT activation

It has been reported that DAG induces Ca^{2+} influx through activation of cation channels (Hofmann *et al*, 1999; Clapham, 2003). As the Ang II-induced periodic increase in $[Ca^{2+}]_i$ likely results from enhanced spontaneous activity of myocytes (which are dependent on extracellular Ca^{2+}; see above), and these were suppressed by DGKβ (Supplementary Figure S1), we next examined whether Ca^{2+} influx is involved in DAG-mediated responses. Treatment of cardiac myocytes with Ang II or with a DAG derivative, 1-oleoyl-2-acyl-*sn*-glycerol (OAG), increased the nuclear translocation of GFP-NFAT4 and NFAT activity, both of which were almost completely suppressed by the voltage-dependent Ca^{2+} channel blocker nitrendipine and a receptor-activated cation channel (RACC) inhibitor SK&F96365 (Figure 3A–C). As OAG-induced NFAT activation was also completely suppressed by cyclosporine A, a calcineurin inhibitor (Figure 3C), DAG increases NFAT activity through calcineurin activation. These results suggest that RACC and Ca^{2+} influx through L-type Ca^{2+} channel mediate Ang II- or DAG-induced NFAT activation.

Ang II activates DAG-sensitive cation channels in cardiac myocytes

To directly demonstrate that Ang II activates DAG-sensitive RACC, whole-cell patch-clamp experiments were performed. In quasi-physiological ionic conditions, administration of Ang II into the bath activated inward currents at −80 mV, which were further enhanced by RHC80267 (Figure 4A and B). These currents were completely abolished by *N*-methyl-D-glucamine substitution for all external cations (data not shown), and showed an outward-rectifying property with the reversal potential of ca. 0 mV (1.0±1.0 mV, $n=6$), when Cs^+ was intracellularly dialyzed via patch pipette and TTX (3 μM) and nitrendipine (1 μM) were added into

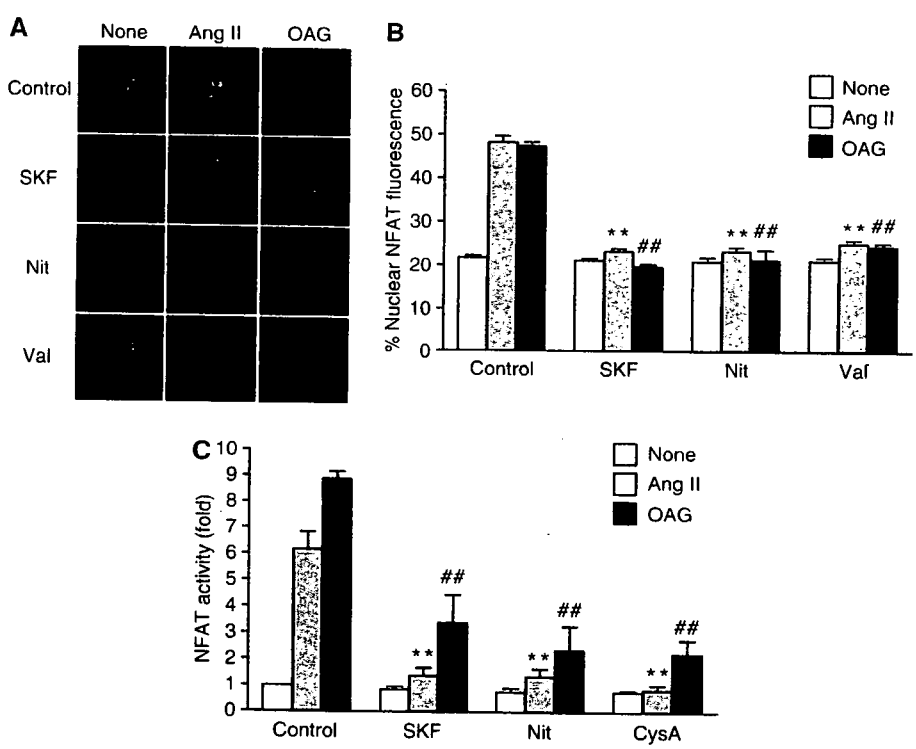

Figure 3 Requirement of RACC and L-type Ca^{2+} channel in DAG-mediated NFAT translocation. (**A**) Effects of SK&F96365 (SKF), nitrendipine (Nit) and valinomycin (Val) on Ang II- or OAG-induced NFAT translocation. (**B**) Quantification of the nuclear predominant fluorescence of GFP-NFAT4 without (None) or with Ang II or OAG stimulation. (**C**) Effects of SKF, Nit, and cyclosporine A (CysA) on Ang II- or OAG-induced increase in NFAT-luciferase activity. Cells were treated with SKF (10 μM), Nit (1 μM), Val (1 μM), or CysA (1 μM) for 30 min before the addition of Ang II (100 nM) or OAG (25 μM). $^{**}P<0.01$ versus Ang II stimulation of control cells. ##; $P<0.01$ versus OAG stimulation of control cells.

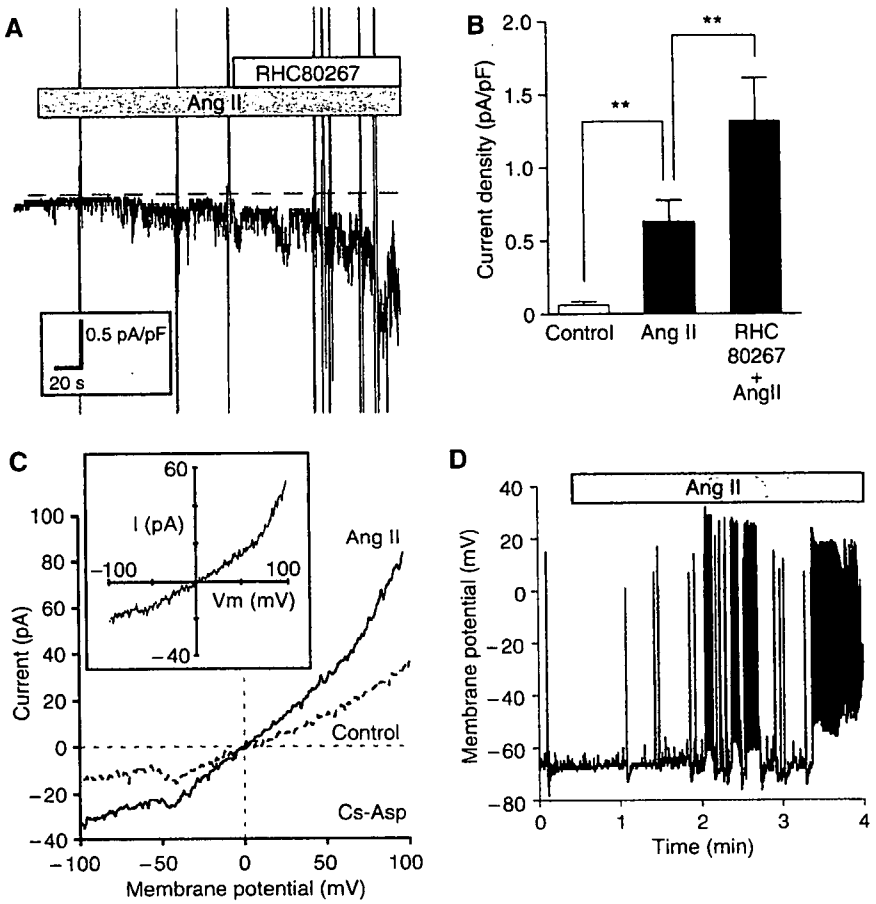

Figure 4 Activation of DAG-sensitive currents from single cardiomyocytes by Ang II stimulation. (**A**) Representative traces of ionic currents recorded from Ang II-treated cardiomyocytes at a holding potential of −80 mV under conventional whole-cell patch-clamp with K^+-internal solution. The nonselective cation currents are activated by Ang II (1 μM), and potentiated by RHC80267 (30 μM). The dotted line represents the zero current level. (**B**) Current density of inward current (at −80 mV) averaged for the period of 60–65 s after Ang II stimulation or RHC80267 treatment ($n>8$). $^{**}P<0.01$. (**C**) *I–V* relationship of ionic currents from unstimulated (Control) and Ang II-stimulated myocytes with Cs^+-internal solution containing myo-IP_3 (10 μM). TTX (3 μM) and nitrendipine (1 μM) are included in the K^+-free external solution. (Inset) *I–V* relationship of TRPC-like currents induced by Ang II (differences between Ang II and Control). (**D**) Representative traces of time-dependent changes in the membrane potential and the frequency of action potential by Ang II stimulation in the current-clamp mode.

K^+-free external solution to block voltage-dependent K^+, Na^+, and L-type Ca^{2+} channels, respectively (see inset in Figure 4C). Administration of OAG (25 μM) also activated inward currents showing indistinguishable properties from those activated by Ang II, whereas application of myo-IP_3 (10 μM) in the internal solution was unable to activate any discernible currents by itself (data not shown). These results collectively suggest that Ang II activates DAG-sensitive nonselective cation currents in cardiomyocytes via an IP_3-independent pathway, which bears considerable resemblance to heterologously expressed TRPC channels.

In the next step, we examined Ang II-induced changes in membrane potential by using the current-clamp technique, since the treatment with valinomycin, a K^+ ionophore, which causes inactivation of voltage-dependent channels via stabilization of membrane potential (Linares-Hernandez *et al*, 1998), completely suppressed the Ang II-induced translocation of GFP-NFAT4 (Figure 3A and B), and in general, the activation of RACC causes membrane depolarization (Large, 2002). As expected, membrane potential recording from single myocytes with current-clamp mode clearly demonstrated that Ang II increased the frequency of action potentials, which eventually led to continuous burstic firing superimposed on concomitant sustained depolarization (22.2 ± 5.6 mV, $n=5$) (Figure 4D). It is noteworthy that the time course of these effects is very similar to that observed for the enhanced frequency of Ca^{2+} oscillations induced by Ang II (see above).

Properties of DAG induced membrane depolarization in rat cardiac myocytes

Current-clamp recordings were technically little feasible to monitor the membrane potential for a long period of time, because of rhythmical contractions of myocytes evoked by Ang II. To circumvent this problem, we adopted a voltage-sensitive fluorescent probe $DiBAC_4(3)$. After $DiBAC_4(3)$ enters the cells, it binds to cellular proteins and membrane lipids. Then, $DiBAC_4(3)$ enhances fluorescence. Because of its slow dissociating nature, $DiBAC_4(3)$ can only detect slow cumulative changes in resting potential rather than rapid changes in membrane potential generated by action potential. Ang II stimulation gradually increased the fluorescence intensity of $DiBAC_4(3)$ (Figure 5A and B), indicating the shift of membrane potential to positive (BACzkó *et al*, 2004). The

averaged changes in membrane potential induced by Ang II were estimated to be ~15 mV. Treatment with RHC80267 enhanced the Ang II-induced increases in the fluorescence intensity of $DiBAC_4(3)$ (Figure 5C). These results indicate that DAG generated by Ang II stimulation shifts the membrane potential of cardiac myocytes more positively. DAG also activates other signaling molecules including protein kinase C (PKC). PKC is known to potentiate the extent of L-type Ca^{2+} channel activation, and both OAG and phorbor 12-myristrate 13-acetate (PMA) have been reported to increase the channel open probability in rat cardiomyocytes (Guinamard *et al*, 2004). However, treatment with PMA did not increase the fluorescence intensity of $DiBAC_4(3)$ (Figure 5A and B) and OAG-induced translocation and activation of NFAT were not affected by bisindolylmaleimide, a selective PKC inhibitor (Supplementary Figure S2). It is possible that

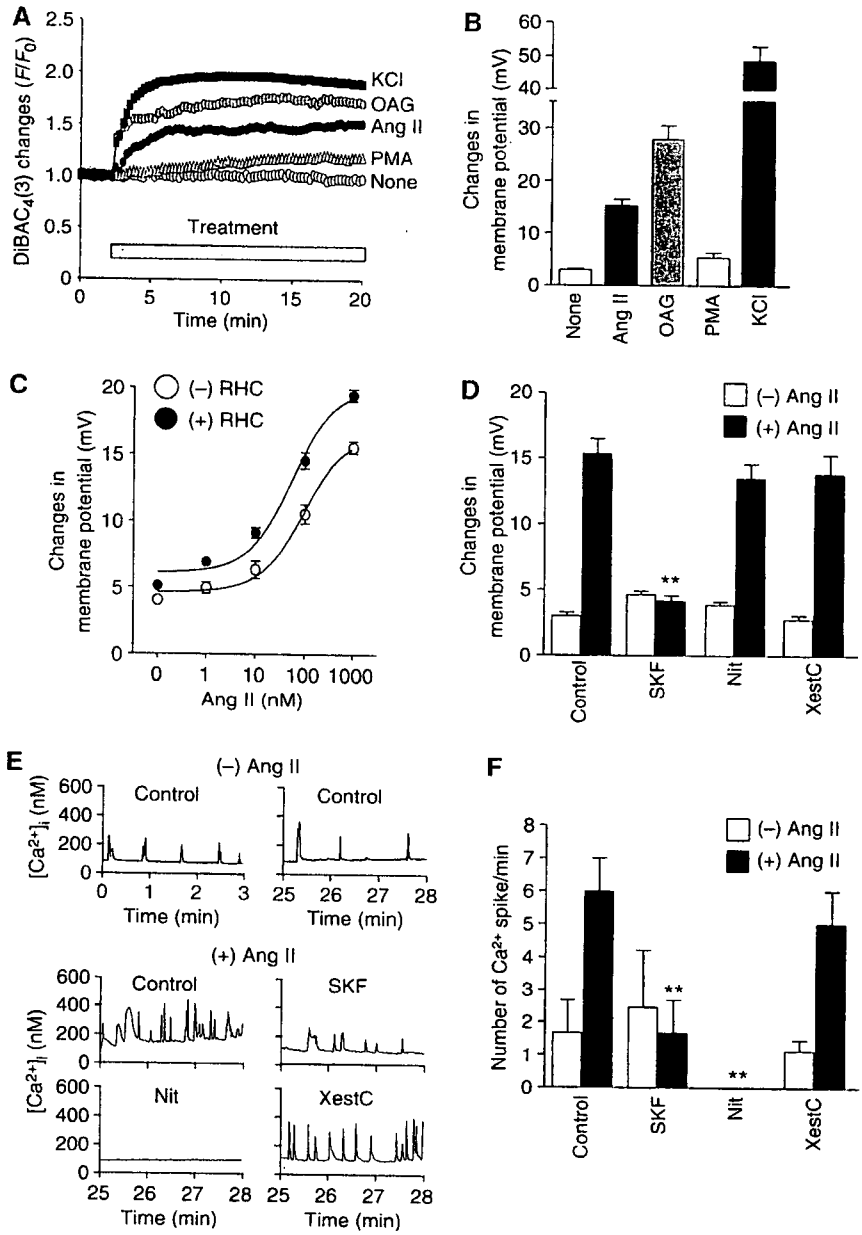

Figure 5 Changes in membrane potential through RACC activation by DAG. (**A**) Representative time courses of changes in Ang II-, OAG-, or PMA-induced F/F_0 of $DiBAC_4(3)$ fluorescence from time course experiments. Cells were stimulated with Ang II (1 μM), OAG (25 μM), PMA (1 μM), or KCl (10 mM). F_0 means the initial value of fluorescence. (**B**) Maximal changes in resting membrane potential calculated from the changes in $DiBAC_4(3)$ fluorescence intensity during 15 min drug treatment. For the *in vivo* calibration of the membrane potentials, the KCl-induced maximal changes in fluorescence were fitted to the theoretical potentials obtained from Nernst equation, and then the changes in membrane potential by Ang II stimulation was calculated based on the fitting fomula. (**C**) Effects of RHC80267 on the concentration-dependent changes in resting membrane potentials induced by Ang II stimulation. (**D**) Involvement of RACC in Ang II-induced increases in the resting membrane potential. Cells were treated with SK&F96365 (SKF, 10 μM), nitredipine (Nit, 1 μM), or xestospongin C (XestC, 20 μM) for 30 min before the addition of Ang II. $^{**}P<0.01$ versus Ang II stimulation of control cells. (**E**) Effects of SK&F96365 (SKF), nitrendipine (Nit), and xestospongin C (XestC) on Ang II-induced Ca^{2+} responses. The digital images were obtained every 1 s during 0–3 min under basal conditions and during 25–28 min after Ang II stimulation. (**F**) Number of Ca^{2+} spikes was normalized to per minute. $^{**}P<0.01$ versus Ang II stimulation of control cells.

the metabolites of DAG work as mediators for NFAT translocation. However, treatment with arachidonic acid (AA) or phospholipase A_2 (PLA_2) inhibitors did not affect Ang II-induced NFAT translocation (Supplementary Figure S2). These results suggest that PKCs and DAG metabolites do not participate in Ang II-induced depolarization and NFAT translocation. The Ang II-induced increases in the fluorescence intensity of $DiBAC_4(3)$ were completely suppressed by SK&F96365, but not by nitrendipine and xestospongin C (Figure 5D).

We next examined whether periodic increase in $[Ca^{2+}]_i$ is regulated by RACC. The myocytes showed spontaneous Ca^{2+} oscillations in the presence of extracellular Ca^{2+} (top panel in Figure 5E). The frequency of Ca^{2+} oscillations was increased by Ang II stimulation and this was suppressed by SK&F96365 and nitrendipine, but not by xestspongin C (middle and bottom panels in Figure 5E and F). These results support the idea that DAG generated by Ang II-induced PLC activation causes membrane depolarization through RACC activation and thereby secondarily activates L-type Ca^{2+} channel, leading to increased frequency of Ca^{2+} oscillations.

Requirement of TRPC3 and TRPC6 in Ang II-induced membrane depolarization

TRPC proteins are thought to be molecular candidates for RACC (Clapham, 2003). We found the expression of at least five TRP canonical (TRPC) mRNAs (TRPC1, TRPC3, TRPC4, TRPC5, TRPC6, and TRPC7) in rat neonatal cardiomyocytes by RT-PCR analysis (data not shown). Recent reports have demonstrated that three TRPC channels (TRPC3, TRPC6, and TRPC7) are activated directly by DAG (Hofmann *et al*, 1999; Clapham, 2003). Thus, we next examined which DAG-sensitive TRPC protein is involved in Ang II-induced NFAT activation. We overexpressed TRPC3, TRPC6, or TRPC7, and examined the Ang II-induced changes in membrane potential with $DiBAC_4(3)$ (Figure 6A and B). Among three TRPC proteins, Ang II-induced increases in the fluorescence intensity of $DiBAC_4(3)$ were significantly enhanced by the expression of TRPC3 and TRPC6 but not by TRPC7 (Figure 6B), although the latter enhanced OAG-induced $[Ca^{2+}]_i$ increases to the same extent as the former two did (Supplementary Figure S3). These results indicate that TRPC3 and TRPC6, but not TRPC7, likely regulate the Ang II-induced membrane depolarization. This conclusion was further corroborated by siRNA-mediated knockdown of TRPC3 (siRNA 1397, 1992, and 2043) and TRPC6 (siRNA 1609 and 1786) in the cardiomyocytes; this procedure decreased the expression level of endogenous TRPC3 and TRPC6 proteins without affecting other TRPC proteins (Figure 6C–F), and simultaneously caused significant suppression of Ang II-induced increases in the fluorescence intensity of $DiBAC_4(3)$ (Figure 6G). Taken together, the above results strongly suggest that DAG-mediated activation of TRPC3 and TRPC6 channels contributes to the enhanced Ca^{2+} oscillation by Ang II via their membrane depolarizing actions.

In addition, siRNA silencing of TRPC3 and TRPC6 also significantly suppressed Ca^{2+} entry-mediated $[Ca^{2+}]_i$ elevation induced by the addition of Ca^{2+} into the bath after Ang II stimulation (Supplementary Figure S3). Thus, some role of direct Ca^{2+} entry via TRPC3/TRPC6-associated pathway cannot completely be excluded in the Ang II-enhanced Ca^{2+} oscillation.

Requirement of TRPC3 and TRPC6 in Ang II-induced NFAT translocation and hypertrophic responses

We next examined whether TRPC3 and TRPC6 are involved in Ang II-induced hypertrophic responses. Treatment with siRNAs of TRPC3 and TRPC6 significantly suppressed Ang II-induced NFAT translocation (Figure 7A and B). Furthermore, both TRPC3 and TRPC6 siRNAs suppressed Ang II-induced actin reorganization and protein synthesis (Figure 7C and D). We further examined the involvement of TRPC6 in Ang II-induced cardiomyocyte hypertrophy by using two dominant negative TRPC6 mutants (Hofmann *et al*, 2002; Hisatsune *et al*, 2004). Expression of TRPC6-Δ(N) and TRPC6-3A significantly suppressed Ang II-induced NFAT activation, actin reorganization, and protein synthesis (Supplementary Figure S4). These results suggest that TRPC3 and TRPC6 play a critical role in Ang II-induced hypertrophic responses in rat neonatal cardiomyocytes.

Discussion

This study reveals the role of DAG in Ang II-induced NFAT activation and hypertrophic responses. DAG produced by Ang II-induced PLC activation directly activates TRPC3 and TRPC6, and the resulting cation (Na^+, Ca^{2+}) influx changes membrane potential to positive, leading to activation of voltage-dependent L-type Ca^{2+} channel possibly through the generation of action potential. The increase in Ca^{2+} influx through L-type Ca^{2+} channel can activate calcineurin/NFAT pathway and hypertrophic responses in rat neonatal cardiomyocytes (Figure 8).

The physiological role of TRPC was first identified in the vascular smooth muscle cells (Inoue *et al*, 2001). In the vascular system, activation of TRPC6 contributes to membrane depolarization and regulates myogenic tone of resistance arteries (Large, 2002; Welsh *et al*, 2002). In the present study, we demonstrated that TRPC3 and TRPC6 activated by DAG contributes to the shift of membrane potential and subsequent Ca^{2+} signal generation through voltage-dependent Ca^{2+} channel in cardiac myocytes. The role of DAG-induced TRPC3 and TRPC6 activation in membrane depolarization has been reported in vascular smooth muscle cells (Reading *et al*, 2005; Soboloff *et al*, 2005). The novel finding of the present study is to characterize the pathophysiological significance of TRPC3 and TRPC6 in Ang II-induced hypertrophic responses of the heart.

We cannot determine the subtype(s) of TRPC proteins activated by Ang II from the *I–V* relationship of native RACC, as inward current activated by Ang II was too small (Figure 4). Previous report has shown that fulfenamate inhibits TRPC3 but enhances TRPC6 channel activity (Inoue *et al*, 2001). The Ang II-induced inward current was slightly inhibited by flufenamate (data not shown). However, the similar behavior of currents to the present study was reported in TRPC3/C6-co-expressing HEK293 cells (Maruyama *et al*, 2006). TRPC3-like currents were observed by coexpression of TRPC3 and TRPC6. As Ang II-induced responses were inhibited both by siRNAs of TRPC3 and TRPC6 (Figures 6 and 7), we speculate that TRPC3 and TRPC6 form heterotetramers to regulate DAG-sensitive native cationic currents in cardiac myocytes.

In our hands, the expression of TRPC7 did not enhance Ang II-induced membrane depolarization (Figure 6B). This

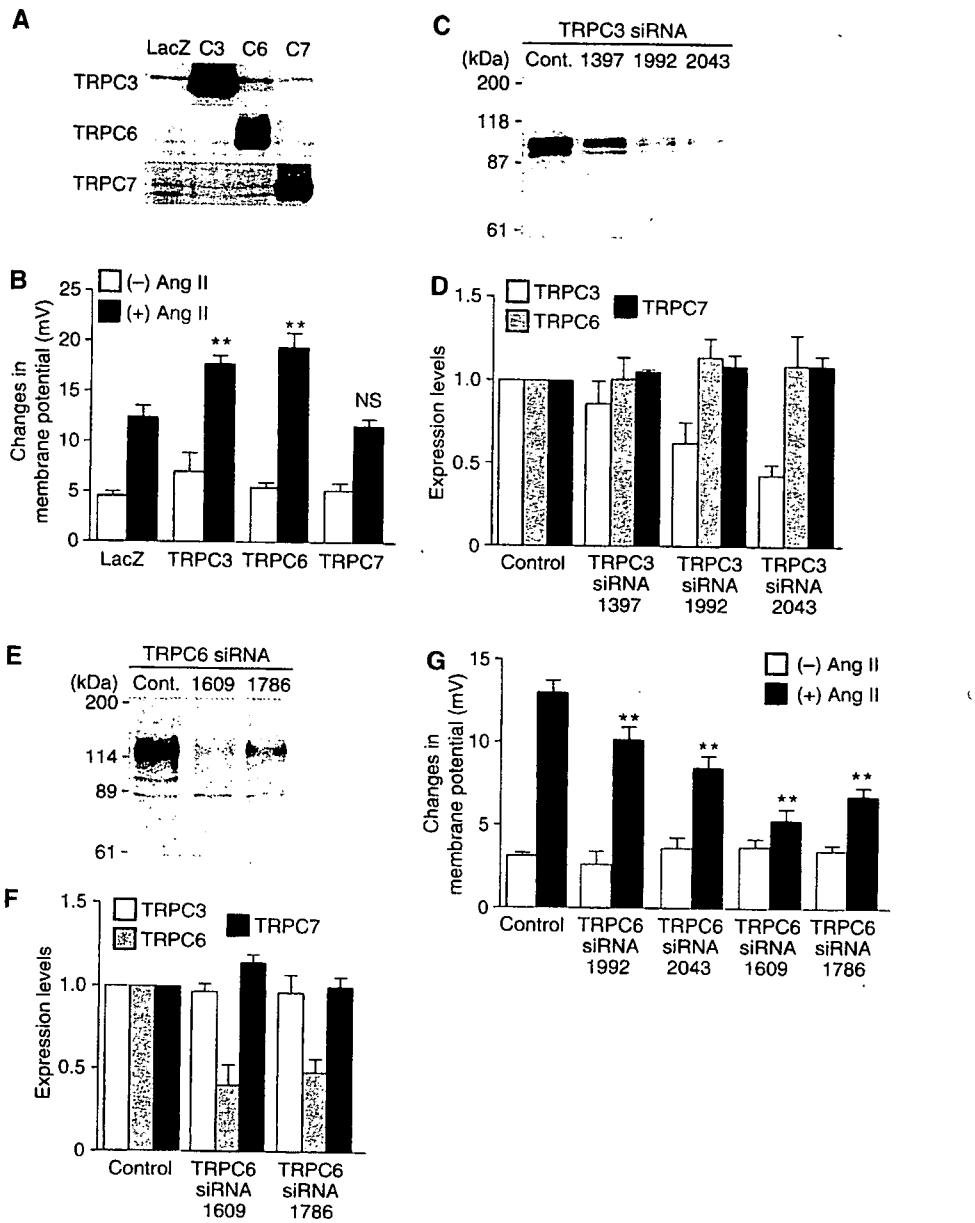

Figure 6 Requirement of TRPC3 and TRPC6 in Ang II-induced increases in membrane potential. (**A**) Western blots of the respective TRPC proteins. To identify the sizes of TRPC3 (C3), TRPC6 (C6), and TRPC7 (C7), each TRPC was overexpressed with recombinant adenoviruses. (**B**) Potentiating effects of TRPC3 and TRPC6 on changes in membrane potential by Ang II stimulation in LacZ-, TRPC3-, TRPC6-, and TRPC7-expressing cells. $^{**}P<0.01$ versus Ang II stimulation of LacZ-expressing cells. NS means no significance from LacZ-expressing cells. (C–F) Effects of TRPC3 siRNAs (**C**, **D**) and TRPC6 siRNAs (**E**, **F**) on the expression of the respective TRPC proteins. (C, E) Representative Western blots with anti-TRPC3 (C) and anti-TRPC6 (E). (D, F) Effects of siRNAs of TRPC3 and TRPC6 on the average expression of native TRPC3, TRPC6, and TRPC7 proteins. (**G**) Effects of siRNAs of TRPC3 and TRPC6 on the maximal changes in $DiBAC_4(3)$ fluorescence intensity by Ang II (100 nM). Data are shown as the changes in membrane potentials (mV) calculated by *in vivo* calibration. $^{**}P<0.01$ versus Ang II stimulation of control siRNA-treated cells (Control).

may be explained by differential spatial organization and dynamics in the receptor-transduction systems (Delmas *et al*, 2002). As OAG-induced increases in $[Ca^{2+}]_i$, but Ang II-induced shift of membrane potential, was not enhanced in TRPC7-expressing cells (Supplementary Figure S3, Figure 6B), Ang II signaling microdomain may contain TRPC6 and TRPC3, but not TRPC7. This idea is supported by the reports that stimulation of AT1R activates TRPC6 (Large, 2002; Winn *et al*, 2005).

Previous report suggested that capacitative Ca^{2+} entry contributes to the nuclear translocation of NFAT and hypertrophy in cardiomyocytes (Hunton *et al*, 2002). In contrast with the present study, they showed that IP_3-mediated store depletion triggers the activation of SOC and activates hypertrophic responses. Although we cannot explain the discrepancy between their report and the present study, we clearly demonstrated that xestospongin C or IP_3-sponge did not affect Ang II-induced changes in fluorescence intensity of $DiBAC_4(3)$, NFAT activation, and hypertrophic responses (Figures 1 and 5D). We also confirmed that the application of high concentration of IP_3 did not activate whole-cell currents (data not shown). In addition, treatment with

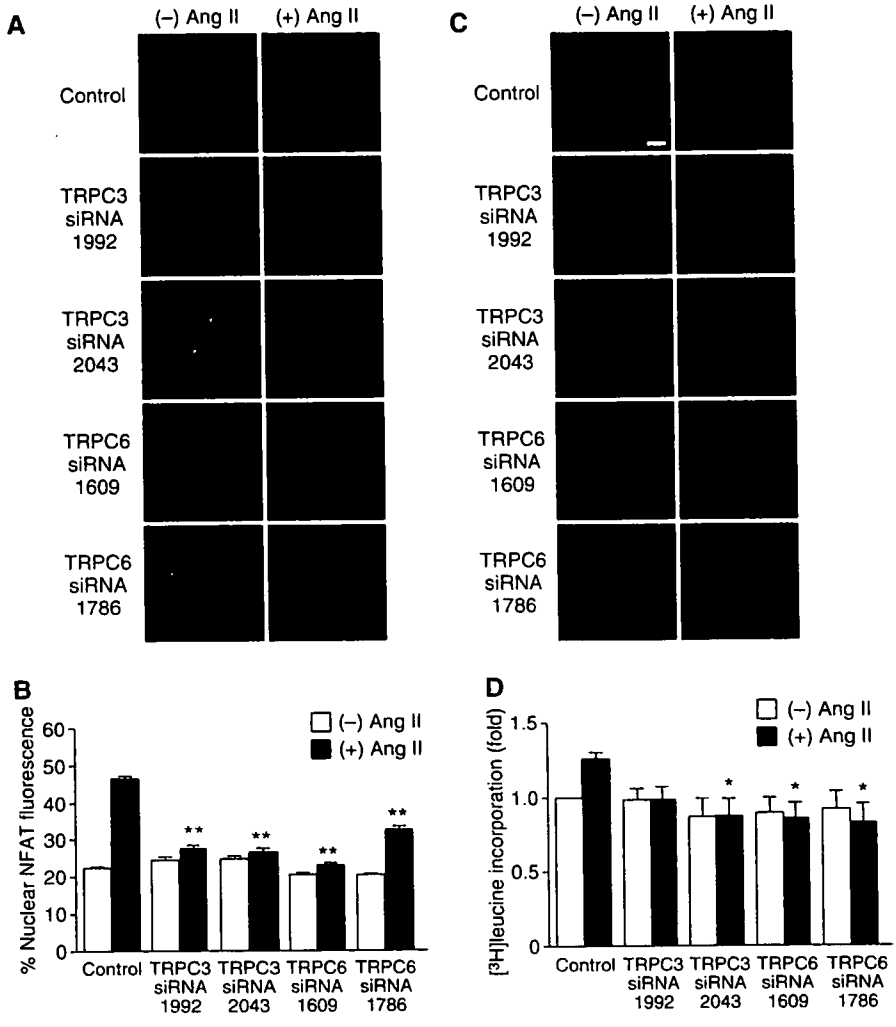

Figure 7 Requirement of TRPC3 and TRPC6 in Ang II-induced hypertrophic responses. Effects of siRNAs of TRPC3 and TRPC6 on Ang II-induced NFAT translocation (**A**, **B**), actin reorganization (**C**), and protein synthesis (**D**). Scale bar = 20 μm. $^{*}P<0.05$, $^{**}P<0.01$ versus Ang II stimulation of control siRNA-treated cells (Control).

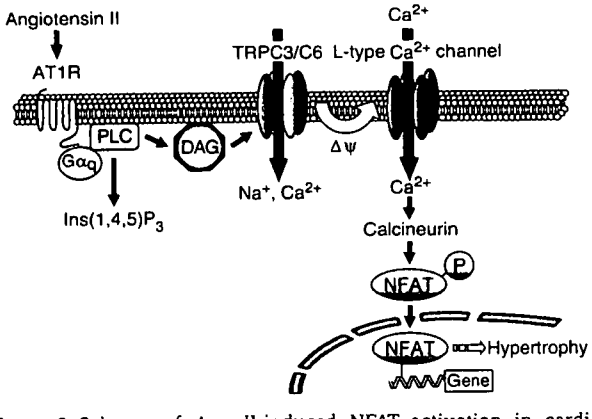

Figure 8 Schema of Ang II-induced NFAT activation in cardiac myocytes. In cardiac myocytes, stimulation of AT1R induces NFAT activation through $G\alpha_q$-PLC signaling pathway. DAG, generated by PLC activation, directly activates TRPC3 and TRPC6 (TRPC3/C6). Activation of TRPC3/C6 causes slow increases in the membrane potential to a positive direction ($\Delta\Psi$) and concomitantly increases the frequency of spontaneous firing due to activation of L-type Ca^{2+} channel. The Ca^{2+} influx though L-type Ca^{2+} channel activates calcineurin-NFAT pathway, which leads to hypertrophic responses in cardiomyocytes.

caged-IP_3 did not affect the localization of GFP-NFAT4 upon UV irradiation, although caged-IP_3 induced a marked increases in $[Ca^{2+}]_i$ (Supplementary Figure 5). We observed that the treatments with thapsigargin and ionomycin induce NFAT activation through store-operated Ca^{2+} influx. However, Ang II-stimulated increase in $[Ca^{2+}]_i$ through IP_3-mediated Ca^{2+} release is 25–30% of those induced by thapsigargin and ionomycin treatment. This IP_3-mediated increase may not be enough for the activation of SOC. These results suggest that IP_3-mediated Ca^{2+} signaling, including SOC, is not responsible for Ang II-induced NFAT activation.

Whole-cell current experiments revealed that the membrane currents were activated more than 1 min after Ang II stimulation (Figure 4A). However, the maximal shift of membrane potential was achieved about 2 min after Ang II stimulation (Figure 5A). The distinct delay may be explained by DAG metabolism, as RHC80267 enhanced Ang II-induced inward current (Figure 4B). The steady-state DAG lipase activity may regulate the time to elevate DAG concentration required for the activation of whole-cell currents and subsequent changes in membrane potential.

Growing evidence has indicated the involvement of L-type Ca^{2+} channels in the induction of cardiac hypertrophy (Lubic *et al*, 1994, 1995; Whitehurst *et al*, 1999; Liao *et al*, 2005). The role of L-type Ca^{2+} channels in excitation-transcription coupling is well established in the nervous system (Dolmetsch *et al*, 2001, 2003). Calmodulin is reported to be critical for conveying the Ca^{2+} signal to the nucleus (Dolmetsch *et al*, 2001). As calmodulin also regulates calcineurin activity, calmodulin may convey the signal to the nucleus in the cardiovascular system in a similar manner to the nervous system.

While this study is in review process, Bush *et al* (2006) reported that TRPC channels are involved in hypertrophy through pathological calcineurin/NFAT signaling. They showed that TRPC3 expression is upregulated in mice with pathological hypertrophy. We demonstrated that TRPC3 and TRPC6 mediate hypertrophic responses of neonatal myocytes by Ang II stimulation. Thus, the upregulated TRPC channels *in vivo* may enhance receptor-stimulated hypertrophy through the mechanism that we have demonstrated in this study.

In summary, we demonstrated for the first time that PLC-generated DAG has a pathophysiological role in activation of TRPC3 and TRPC6, and TRPC3/6 mediates NFAT-mediated hypertrophic responses through L-type Ca^{2+} channel.

Materials and methods

Materials, plasmid construction, and cell cultures

AT1R blocker CV11974 was provided from Takeda Chemical Industries Ltd (Osaka, Japan). PTX, SK&F96365, caged-IP_3, and $cPLA_2$ inhibitor were purchased from Calbiochem. Valinomycin, cyclosporine A, U73122, U73343, AA, $PACOCF_3$, myo-IP_3, TTX, and PD123319 were from Sigma. Fura2/AM was from Dojindo. Collagenase, Liberase (enzyme 3), and Fugene 6 were from Roche. Alexa Fluor 594-phalloidin and $DiBAC_4(3)$ were from Molecular Probe. Nitrendipine was from Wako. The cDNA coding DGKβ (KIAA0718) was obtained from Kazusa DNA Research Institute. The cDNAs coding mouse TRPC3, TRPC6, and TRPC7, and anti-TRPC7 antibody were prepared as described (Inoue *et al*, 2001; Nishida *et al*, 2003). Anti-TRPC6 and anti-TRPC3 antibodies were from Alomone. Mouse TRPC6-3A and TRPC6-Δ(N) were constructed according to the previous reports (Hofmann *et al*, 2002; Hisatsune *et al*, 2004). The cDNA coding IP_3-sponge was cloned from mouse brain (Uchiyama *et al*, 2002), and GFP-IP_3-sponge was constructed in pEGFP-C1 vector (Clontech). Isolation of rat neonatal cardiomyocytes was described (Nishida *et al*, 2000).

Production of adenoviruses, infection, and transfection

Recombinant adenoviruses of GFP-NFAT4, HA-tagged DGKβ, GFP-DGKβ, wild-type TRPC6, TRPC6-3A, TRPC6-Δ(N), and GFP-fused IP_3-sponge (GFP-IP_3-sponge) were produced by the method of He *et al* (1998) with a slight modification. Other adenoviruses were prepared as described previously (Nishida *et al*, 2000, 2005; Arai *et al*, 2003). Cells were infected with adenovirus(es) at 100 MOI for 48 h. Small interference RNAs (250 nM) were transfected with lipofectamine 2000 for 72 h.

Measurement of NFAT activity

Measurement of NFAT activity was performed as described previously (Fujii *et al*, 2005). At 2 h after adenoviral infection in serum-free medium, cardiomyocytes (1×10^6 cells) plated on 24-well dishes were transiently cotransfected with 0.45 μg pNFAT-Luc and 0.05 μg pRL-SV40 control plasmid, using Fugene 6. For measuring the translocation of GFP-NFAT4, cells (1×10^6) plated on glass-bottom 35 mm dishes were infected for 48 h with adenovirus coding GFP-NFAT4 at 100 MOI. After Ang II stimulation (100 nM) for 30 min, the localization of GFP-NFAT4 was determined with a Laser Scanning Confocal Imaging System (Carl Zeiss LSM510) as described (Fujii *et al*, 2005).

Measurement of $[Ca^{2+}]_i$ and membrane potential

The intracellular Ca^{2+} concentration ($[Ca^{2+}]_i$) of cardiomyocytes was determined as described (Arai *et al*, 2003; Nishida *et al*, 2005). Briefly, cells (1×10^6) were plated on gelatin-coated glass-bottom 35 mm dishes and were loaded with 2.5 μM fura-2/AM at 37°C for 30 min. For measurement of cell membrane potential, cells were loaded with 1.5 μM $DiBAC_4(3)$ at 37°C for 30 min. The fluorescence intensity of $DiBAC_4(3)$ was measured at an excitation wavelength of 488 nm with a video image analysis system (Aquacosmos, Hamamatsu Photonics). The peak changes ($\Delta F/F_0$) of $DiBAC_4(3)$ fluorescence intensity were defined as values obtained by subtracting the basal fluorescence intensity (F_0) from the maximal intensity during 19 min Ang II treatment.

Measurement of the expression of TRPC proteins

Cardiomyocytes (3×10^6 cells) plated on six-well dishes were directly harvested with 2 × SDS sample buffer. The protein samples were fractionated by 8% SDS–PAGE gel and then transferred onto PVDF membrane. The expression of endogenous TRPC proteins was assessed by Western blotting using anti-TRPC antibodies. To examine the involvement of TRPC3 and C6, knockdown experiments using siRNAs were performed (sequences of siRNAs used in this study were presented in Supplementary Table 1). We used Stealth (Invitrogen) siRNA sequence to eliminate nonspecific responses by siRNA. Transfection was performed by lipofectamine 2000.

Measurement of hypertrophic responses of cardiomyocytes

Measurement of cardiomyocyte hypertrophy was performed as described (Maruyama *et al*, 2002). Briefly, 24 h after infection, cardiomyocytes were stimulated with Ang II (100 nM) for 48 h. The cells were washed, fixed, and then stained with Alexa Fluor 594-phalloidin to visualize actin filaments. Protein synthesis was measured by [^{3}H]leucine incorporation. After cells were stimulated with Ang II (100 nM) for 18 h, [^{3}H]leucine (1 μCi/ml) was add to the culture medium and further incubated for 6 h. The incorporated [^{3}H]leucine was measured using liquid-scintillation counter.

Electrophysiology

Single neonatal rat cardiac myocytes plated on thin coverslips for 1–2 days (3 × 10 mm; Matsunami, Japan) were used for patch-clamp experiments. The details of patch-clamp experiments are described elsewhere (Shi *et al*, 2004). Internal solution used for the whole-cell variant of patch clamp; K^+-internal solution (mM): 140 K^+, 4 Na^+, 2 Mg^{2+}, 144 Cl^-, 2 EGTA, 2 ATP, 10 HEPES or Cs^+-internal solution (mM): 140 Cs^+, 2 Mg^{2+}, 20 Cl^-, 2 SO_4^{2-}, 120 aspartate, 2 ATP, 5 EGTA (2 Ca^{2+} added), 10 HEPES, and 10 μM myo-IP_3. For current-clamp recordings, normal external solution and K^+-internal solution of the same composition as used for whole-cell voltage-clamp experiments were used. All experiments were performed at 25–28°C with the aid of a temperature control unit (Warner Instruments) to facilitate the response to Ang II.

Statistical analysis

The results are shown as means±s.e.m. All experiments were repeated at least three times. Mean values were compared with control by Student's *t*-test (for two groups) or one-way ANOVA followed by Dunnett's *t*-test (for three or more groups).

Supplementary data

Supplementary data are available at *The EMBO Journal* Online (http://www.embojournal.org).

Acknowledgements

We thank Y Ito (Department of Pharmacology, Graduate School of Medical Sciences, Kyushu University) for using Aquacosmos imaging system during early stage of this study. We also thank SM Lanier and M Sato (Louisiana State University Health Science Center) for experimental suggestion, and T Murakami for DNA construction. This work was supported by grants from the Ministry of Education, Culture, Sports, Science and Technology of Japan (to M Nishida and H Kurose), from Ministry of Health, Labour and Welfare of Japan, and the National Institute of Biomedical

Innovation (MF-16, to YS), and by grants from The Naito Foundation, The Kanae Foundation, The Suzuken Memorial Foundation, The Uehara Memorial Foundation, Kao Foundation for Arts and Sciences, Takeda Science Foundation and Japan Heart Foundation Research Grant (to MN), and Astellas Foundation for Research on Metabolic Disorders (H Kurose).

References

Arai K, Maruyama Y, Nishida M, Tanabe S, Takagahara S, Kozasa T, Mori Y, Nagao T, Kurose H (2003) Endothelin-1-induced MAPK activation and cardiomyocyte hypertrophy are mediated by $G\alpha_{12}$ and $G\alpha_{13}$ as well as $G\alpha_q$ and $G\beta\gamma$ subunits. *Mol Pharmacol* **63**: 478–488

BACzkó I, Giles WR, Light PE (2004) Pharmacological activation of plasma-membrane K_{ATP} channels reduces reoxygenation-induced Ca^{2+} overload in cardiac myocytes via modulation of the diastolic membrane potential. *Br J Pharmacol* **141**: 1059–1067

Bush EW, Hood DB, Papst PJ, Chapo JA, Minobe W, Bristow MR, Olson EN, McKinsey TA (2006) TRPC channels promote cardiomyocyte hypertrophy through activation of calcineurin signaling. *J Biol Chem*, (in press) (doi: 10.1074/jbc.M605536200)

Clapham DE (2003) TRP channels as cellular sensors. *Nature* **426**: 517–524

Crabtree GR, Olson EN (2002) NFAT signaling: choreographing the social lives of cells. *Cell* **109**: S67–S79

Delmas P, Wanaverbecq N, Abogadie FC, Mistry M, Brown DA (2002) Signaling microdomains define the specificity of receptor-mediated InsP3 pathways in neurons. *Neuron* **34**: 209–220

Dolmetsch R (2003) Excitation-transcription coupling: signaling by ion channels to the nucleus. *Science's stke*, www.stke.org/cgi/content/full/sigtrans;2003/166/pe4

Dolmetsch RE, Lewis RS, Goodnow CC, Healy JI (1997) Differential activation of transcription factors induced by Ca^{2+} response amplitude and duration. *Nature* **386**: 855–858

Dolmetsch RE, Pajvani U, Fife K, Spotts JM, Greenberg ME (2001) Signaling to the nucleus by an L-type calcium channel-calmodulin complex through the MAP kinase pathway. *Science* **294**: 333–339

Dostal DE, Rothblum KN, Chernin MI, Cooper GR, Baker KM (1992) Intracardiac detection of angiotensinogen and renin: a localized rennin–angiotensin system in neonatal rat heart. *Am J Physiol* **263**: C838–C850

Fujii T, Onohara N, Maruyama Y, Tanabe S, Kobayashi H, Fukutomi M, Nagamatsu Y, Nishihara N, Inoue R, Sumimoto H, Shibasaki F, Nagao T, Nishida M, Kurose H (2005) $G\alpha_{12/13}$-mediated production of reactive oxygen species is critical for angiotensin receptor-induced NFAT activation in cardiac fibroblasts. *J Biol Chem* **280**: 23041–23047

Guinamard R, Chatelier A, Lenfant J, Bois P (2004) Activation of the Ca^{2+}-activated nonselective cation channel by diacylglycerol analogues in rat cardiomyocytes. *J Cardiovas Electrophysiol* **15**: 342–348

He TC, Zhou S, da Costa LT, Yu J, KInzler KW, Vogelstein B (1998) A simplified system for generating recombinant adenoviruses. *Proc Natl Acad Sci USA* **95**: 2509–2514

He Y, Yao G, Savoia C, Touyz RM (2005) Transient receptor potential melastatin 7 ion channels regulate magnesium homeostasis in vascular smooth muscle cells. Role of angiotensin II. *Circ Res* **96**: 207–215

Hisatsune C, Kuroda Y, Nakamura K, Inoue T, Nakamura T, Michikawa T, Mizutani A, Mikoshiba K (2004) Regulation of TRPC6 channel activity by tyrosine phosphorylation. *J Biol Chem* **279**: 18887–18894

Hofmann T, Obukhov AG, Schaefer M, Harteneck C, Gudermann T, Schultz G (1999) Direct activation of human TRPC6 and TRPC3 channels by diacylglycerol. *Nature* **397**: 259–263

Hofmann T, Schaefer M, Schultz G, Gudermann T (2002) Subunit composition of mammalian transient receptor potential channels in living cells. *Proc Natl Acad Sci USA* **99**: 7461–7466

Hunton DL, Lucchesi PA, Pang Y, Cheng X, Dell'Italia LJ, Marchase RB (2002) Capacitative calcium entry contributes to nuclear factor of activated T cells nuclear translocation and hypertrophy in cardiomyocytes. *J Biol Chem* **277**: 14266–14273

Inoue R, Okada T, Onoue H, Hara Y, Shimizu S, Naitoh S, Ito Y, Mori Y (2001) The transient receptor potential protein homologue TRP6 is the essential component of vascular α_1-adrenoceptor-activated Ca^{2+}-permeable cation channel. *Circ Res* **88**: 325–332

Large WA (2002) Receptor-operated Ca^{2+}-permeable nonselective cation channels in vascular smooth muscle: a physiologic perspective. *J Cardiovas Electrophysiol* **13**: 493–501

Liao Y, Asakura M, Takashima S, Kato H, Asano Y, Shintani Y, Minamino T, Tomoike H, Hori M, Kitakaze M (2005) Amlodipine ameliorates myocardial hypertrophy by inhibiting EGFR phosphorylation. *Biochem Biophys Res Commun* **327**: 1083–1087

Linares-Hernandez L, Guzman-Grenfell AM, Hicks-Gomez JJ, Gonzalez-Martinez MT (1998) Voltage dependent calcium influx in human sperm assessed by spontaneous detection of intracellular calcium and membrane potential. *Biochem Biophys Acta* **1372**: 1–12

Lubic SP, Giacomini KM, Giacomini JC (1994) Increased 1,4-dihydropyridine binding sites in serum-stimulated cardiomyocytes hypertrophy. *J Pharmacol Exp Ther* **270**: 697–701

Lubic SP, Giacomini KM, Giacomini JC (1995) The effects of modulation of calcium influx through the voltage-sensitive calcium channel on cardiomyocyte hypertrophy. *J Mol Cell Cardiol* **27**: 917–925

Maruyama Y, Nakanishi Y, Walsh EJ, Wilson DP, Welsh DG, Cole WC (2006) Heteromultimeric TRPC6-TRPC7 channels contribute to arginine vasopressin-induced cation current of A7r5 vascular smooth muscle cells. *Circ Res* **98**: 1520–1527

Maruyama Y, Nishida M, Sugimoto Y, Tanabe S, Turner JH, Kozasa T, Wada T, Nagao T, Kurose H (2002) $G\alpha_{12/13}$ mediate α_1-adrenergic receptor-induced cardiac hypertrophy. *Circ Res* **91**: 961–969

Molkentin JD, Dorn II GW (2001) Cytoplasmic signaling pathways that regulate cardiac hypertrophy. *Annu Rev Physiol* **63**: 391–426

Molkentin JD, Lu JR, Antos CL, Markham B, Richardson J, Robbins J, Grant SR, Olson EN (1998) A calcineurin-dependent transcriptional pathway for cardiac hypertrophy. *Cell* **93**: 215–228

Moschella MC, Marks AR (1993) Inositol 1,4,5-trisphosphate receptor expression in cardiac myocytes. *J Clin Invest* **120**: 1137–1146

Nishida M, Maruyama Y, Tanaka R, Kontani K, Nagao T, Kurose H (2000) $G\alpha_i$ and $G\alpha_o$ are target proteins of reactive oxygen species. *Nature* **408**: 492–495

Nishida M, Sugimoto K, Hara Y, Mori E, Morii T, Kurosaki T, Mori Y (2003) Amplification of receptor signalling by Ca^{2+} entry-mediated translocation and activation of PLCγ2 in B lymphocytes. *EMBO J* **22**: 4677–4688

Nishida M, Tanabe S, Maruyama Y, Mangmool S, Urayama K, Nagamatsu Y, Takagahara S, Turner JH, Kozasa T, Kobayashi H, Sato Y, Kawanishi T, Inoue R, Nagao T, Kurose H (2005) $G\alpha_{12/13}$- and reactive oxygen species-dependent activation of c-Jun NH_2-terminal kinase and p38 MAPK by angiotensin receptor stimulation in rat neonatal cardiomyocytes. *J Biol Chem* **280**: 18434–18441

Reading SA, Early S, Waldron BJ, Welsh DG, Brayden JE (2005) TRPC3 mediates pyrimidine receptor-induced depolarization of cerebral arteries. *Am J Physiol* **288**: H2055–H2061

Sadoshima J, Xu Y, Slayter HS, Izumo S (1993) Autocrine release of angiotensin II mediates stretch-induced hypertrophy of cardiac myocytes *in vitro*. *Cell* **75**: 977–984

Seth M, Sumbilla C, Mullen SP, Lewis D, Klein G, Hussain A, Soboloff J, Gill DL, Inesi G (2004) Sarco(endo)plasmic reticulum Ca^{2+} ATPase (SERCA) gene silencing and remodeling of the Ca^{2+} signaling mechanism in cardiac myocytes. *Proc Natl Acd Sci USA* **101**: 16683–16688

Shi J, Mori E, Mori Y, Mori M, Li J, Ito Y, Inoue R (2004) Multiple regulation by calcium of murine homologues of transient receptor potential proteins TRPC6 and TRPC7 expressed in HEK293 cells. *J Physiol* **561**: 415–432

Soboloff J, Spassova M, Xu W, He LP, Cuesta N, Gill DL (2005) Role of endogenous TRPC6 channels in Ca^{2+} signal generation in A7r5 smooth muscle cells. *J Biol Chem* **280**: 39786–39794

Taigen T, De Windt LJ, Lim HW, Molkentin JD (2000) Targeted inhibition of calcineurin prevents agonist-induced cardiomyocyte hypertrophy. *Proc Natl Acd Sci USA* **97**: 1196–1201

Timmerman LA, Clipstone NA, Ho SN, Northrop JP, Crabtree GR (1996) Rapid shuttling of NF-AT in discrimination of Ca^{2+} signals and immunosuppression. *Nature* **383:** 837–840

Tomida T, Hirose K, Takizawa A, Shibasaki F, Iino M (2003) NFAT functions as a working memory of Ca^{2+} signals in decoding Ca^{2+} oscillation. *EMBO J* **22:** 3825–3832

Touyz RM, He Y, Montezano ACI, Yao G, Chubanov V, Gudermann T, Callera GE (2006) Differential regulation of transient receptor potential melastatin 6 and 7 cation channels by ANG II in vascular smooth muscle cells from spontaneous hypertensive rats. *Am J Physiol* **290:** R73–R78

Uchiyama T, Yoshikawa F, Hishida A, Furuichi T, Mikoshiba K (2002) A novel recombinant hyperaffinity inositol 1,4,5 -trisphosphate (IP_3) absorbent traps IP_3, resulting in specific inhibition of IP_3-mediated calcium signaling. *J Biol Chem* **277:** 8106–8113

Welsh DG, Morielli AD, Nelson MT, Brayden JE (2002) Transient receptor potential channels regulate myogenic tone of resistance arteries. *Circ Res* **90:** 248–250

Whitehurst Jr RM, Zhang M, Bhattacharjee A, Li M (1999) Dexamethasone-induced hypertrophy in rat neonatal cardiac myocytes involves an elevated L-type Ca^{2+} current. *J Mol Cell Cardiol* **31:** 1551–1558

Wilkins BJ, De Windt LJ, Bueno OF, Braz JC, Glascock BJ, Kimball TF, Molkentin JD (2002) Targeted disruption of NFATc3, but not NFATc4, reveals an intrinsic defect in calcineurin-mediated cardiac hypertrophic growth. *Mol Cell Biol* **22:** 7603–7613

Wilkins BJ, Molkentin JD (2004) Calcium-calcineurin signaling in the regulation of cardiac hypertrophy. *Biochem Biophys Res Commun* **322:** 1178–1191

Winn MP, Conlon PJ, Lynn KL, Farrington MK, Creazzo T, Hawkins AF, Daskalakis N, Kwan SY, Ebersviller S, Burchette JL, Pericak-Vance MA, Howell DN, Vance JM, Rosenberg PB (2005) A mutation of TRPC6 cation channel causes familial focal segmental glomerulosclerosis. *Science* **308:** 1801–1804

Woodcock EA, Matkovich SJ (2005) $Ins(1,4,5)P_3$ receptors and inositol phosphates in the heart-evolutionary artifacts or active signal transducers? *Pharmacol Therap* **107:** 240–251

J Pharmacol Sci 101, 144 – 150 (2006)

Journal of Pharmacological Sciences

Full Paper

Heterotrimeric G Protein $G\alpha_{13}$-Induced Induction of Cytokine mRNAs Through Two Distinct Pathways in Cardiac Fibroblasts

Yuichi Nagamatsu[1], Motohiro Nishida[1], Naoya Onohara[1], Masashi Fukutomi[1], Yoshiko Maruyama[2], Hiroyuki Kobayashi[1], Yoji Sato[3], and Hitoshi Kurose[1,*]

[1]*Department of Pharmacology and Toxicology, Graduate School of Pharmaceutical Sciences, Kyushu University, Fukuoka 812-8582, Japan*
[2]*Laboratory of Cellular Signaling, Graduate School of Pharmaceutical Sciences, University of Tokyo, Tokyo 113-0033, Japan*
[3]*National Institute of Health Sciences, Tokyo 158-8501, Japan*

Received December 14, 2005; Accepted April 17, 2006

Abstract. Overexpression of constitutively active (CA)-$G\alpha_{13}$ significantly increased the expression of interleukin (IL)-1β and IL-6 mRNAs and proteins in rat cardiac fibroblasts. IL-1β mRNA induction by CA-$G\alpha_{13}$ was suppressed by diphenyleneiodonium (DPI), an NADPH oxidase inhibitor, but not by BAPTA-AM, an intracellular Ca^{2+} chelator. In contrast, IL-6 mRNA induction by CA-$G\alpha_{13}$ was suppressed by BAPTA-AM but not by DPI. However, both IL-1β and IL-6 mRNA induction was suppressed by nuclear factor κB (NF-κB) inhibitors. The CA-$G\alpha_{13}$-induced NF-κB activation was suppressed by DPI and BAPTA-AM, but not C3 toxin and the Rho-kinase inhibitor Y27632. IL-6 mRNA induction by CA-$G\alpha_{13}$ was suppressed by SK&F96365 (1-[β-[3-(4-methoxyphenyl)propoxy]-4-methoxyphenethyl]-1*H*-imidazole hydrochloride), an inhibitor of receptor-activated nonselective cation channels, and the expression of CA-$G\alpha_{13}$ increased basal Ca^{2+} influx. These results suggest that $G\alpha_{13}$ regulates IL-1β mRNA induction through the reactive oxygen species-NF-κB pathway, while it regulates IL-6 mRNA induction through the Ca^{2+}-NF-κB pathway.

Keywords: cardiac fibroblast, $G\alpha_{13}$ protein, nuclear factor of κB, Ca^{2+}, interleukin

Introduction

Cardiac fibroblasts play a central role in maintaining extracellular matrix in the normal heart (1). These cells also mediate inflammatory and fibrotic myocardial remodeling in the injured and failing heart. Cardiac fibroblasts serve as intermediate sensors and amplifiers of signals from immune cells and myocytes through production of autocrine and paracrine mediators such as cytokines, growth factors, prostaglandins, and nitric oxide (1 – 5). These mediators induce cardiac hypertrophy and transition of cardiomyocytes to fibroblast phenotype, causing cardiac dysfunction (1, 2).

Interleukins, such as interleukin-1β (IL-1β) or IL-6, are humoral factors that elicit hypertrophy of cardiomyocytes and hyperplasia of cardiac fibroblasts (4 – 9). In these cells, receptor stimulation such as angiotensin (Ang) II (8) or endothelin-1 (9) increases IL-6 expression, and stimulation of β-adrenergic receptor (4) or 5-hydroxytryptamine 2B (5-HT_{2B}) receptor (5) increases IL-1β. These cytokines regulate phenotype and functions of the heart in autocrine and paracrine manners. Recent studies have suggested that these indirect actions are the major mechanism by which Ang II controls cardiac fibroblasts (2, 8). We have previously reported that stimulation of Ang II receptor activates the α subunit of heterotrimeric $G_{12/13}$ proteins ($G\alpha_{12/13}$), leading to production of reactive oxygen species (ROS) through Rac-dependent activation of NADPH oxidase and that $G\alpha_{12/13}$ mediate activation of nuclear factor of activated T cells (NFAT) in rat cardiac fibroblasts (10). As NFAT is reported to regulate IL-6 mRNA induction in vascular smooth muscle cells (11), $G\alpha_{12/13}$ signaling is

*Corresponding author. kurose@phar.kyushu-u.ac.jp
Published online in J-STAGE: June 15, 2006
doi: 10.1254/jphs.FP0051036

assumed to participate in induction of cytokine mRNA in cardiac fibroblasts. However, it has not been examined whether $G\alpha_{12/13}$ actually regulate cytokine mRNA induction in cardiac fibroblasts.

The G_{12} family G proteins, G_{12} and G_{13}, couple with various G protein-coupled receptors and mediate physiological responses by interacting with different signaling proteins (12). The involvement of $G\alpha_{12/13}$ in cardiac hypertrophy by receptor stimulation has been well recognized as the stimulation of α_1-adrenergic receptor (13), endothelin-1 receptor (14), or Ang II receptor (15) induces hypertrophy through $G\alpha_{12/13}$-dependent activation of c-Jun NH_2-terminal kinase (JNK). However, the physiological role of $G\alpha_{12/13}$ signaling in cardiac fibroblasts has not been established.

In this study, we examine whether $G\alpha_{12/13}$ participate in the induction of IL-1β and IL-6 mRNAs in cardiac fibroblasts by expressing constitutively active (CA) mutants of $G\alpha_{12}$ and $G\alpha_{13}$. This study is the first report to demonstrate that activated $G\alpha_{13}$, but not $G\alpha_{12}$, increases IL-1β and IL-6 mRNAs expression through NF-κB-dependent, but Rho-independent mechanisms in cardiac fibroblasts. We further demonstrate that IL-1β mRNA induction by CA-$G\alpha_{13}$ requires ROS, and IL-6 mRNA induction by CA-$G\alpha_{13}$ requires the increase in basal Ca^{2+} influx.

Materials and Methods

Materials and recombinant adenoviruses

BAPTA-AM, cyclosporine A, and Y27632 were purchased from Calbiochem-Novabiochem Co. (San Diego, CA, USA). Catalase, diphenyleneiodonium (DPI), and 1-[β-[3-(4-methoxyphenyl)propoxy]-4-methoxyphenethyl]-1*H*-imidazole hydrochloride (SK&F96365) were purchased from Sigma-Aldrich (St. Louis, MO, USA). 6-(Phenylsulfinyl)tetrazolo[1,5-*b*] pyridazine (Ro-106-9920) was from Tocris Cookson, Ltd. (Bristol, UK). Dulbecco's Modified Eagle's medium (DMEM) and penicillin/streptomycin were from Invitrogen Co. (Carlsbad, CA, USA) Fura2/AM was from Dojindo (Kumamoto). Collagenase and FuGENE 6 were from Roche Diagnostics (Mannheim, Germany). Dual-luciferase Reagents were from Promega Co. (Madison, WI, USA). pNF (nuclear factor)-κB-Luc and pRL-SV40 were from Stratagene Co. (La Jolla, CA, USA) Recombinant adenoviruses of CA-$G\alpha_q$ (R183C), CA-$G\alpha_{12}$ (Q229L), CA-$G\alpha_{13}$ (Q226L), C3 toxin, and IκBα mutant were produced as described previously (10, 15).

Cell culture

Cardiac fibroblasts were prepared from ventricles of 1 – 2-day-old Sprague-Dawley rats, as described previously (16). Briefly, after digestion of ventricles with 0.1% collagenase, isolated fibroblasts were plated on a non-coated dish in DMEM containing 10% fetal bovine serum and 50 U/ml penicillin/streptomycin. Sub-confluent cells were serum-starved for 48 h and used for the experiments.

Measurement of IL-1β and IL-6 mRNAs expression

Three hours after adenoviral infection (300 multiplicity of infection (MOI)) in serum-free medium, fibroblasts (3×10^5 cells) in 6 well dishes were treated with the chemical inhibitors indicated in the figures. Total RNA was extracted 36 h after infection with RNeasy Mini Kit (Qiagen, Inc., Valencia, CA, USA) and RNase-free DNase set (Qiagen), and then 150 ng (in the case of IL-1β and IL-6) or 5 pg (in the case of 18 S rRNA) of total RNA was subjected to real-time reverse transcriptase PCR (RT-PCR) for quantitative measurement. Oligonucleotide primers and fluorescent-labeled TaqMan® probes were designed with Primer Express software (Applied Biosystems, Foster City, CA, USA). IL-1β (forward primer, 5'-GATGATGACGACCTGCTAGTG TGT-3'; reverse primer, 5'-GACAGCACGAGGCAT TTTTGT-3'; TaqMan® probe, 5'-ATTAGACAGCTG CACTGCAGGCTTCGAGAT-3'), IL-6 (forward primer, 5'-CAACTTCCAATGCTCTCCTAATGG-3'; reverse primer, 5'-CCGAGTAGACCTCATAGTGACC TTT-3'; TaqMan® probe, 5'-TCACAGAAGGAGTGG CTAAGGACCAAGACC-3'), TaqMan® 18 S rRNA primers, and a 5'-VIC™-labelled probe were used according to the manufacturer's instructions (Applied Biosystems). All reactions were performed in TaqMan® One-Step RT-PCR Master Mix Reagents (Applied Biosystems) and the Applied Biosystems 7500 Real-Time PCR System (Applied Biosystems). The 18 S ribosomal RNA was used as an internal control to normalize the differences in the amount of total RNA in each sample.

ELISA for IL-1β and IL-6

ELISA kits for Rat IL-1β and IL-6 were purchased from Pierce (Rockford, IL, USA) and Immuno-Biological Laboratories (Hamburg, Germany), respectively. Assays were performed according to the manufacturer's instructions.

Measurement of NF-κB activation

Two hours after adenoviral infection (100 MOI) in serum-free medium, fibroblasts (3×10^5 cells) in 24-well dishes were transiently co-transfected with 0.45 μg pNF-κB-Luc and 0.05 μg pRL-SV40 control plasmid, using Fugene 6 (10). Luciferase activity was measured 48 h after transfection with Dual-luciferase Reagents.

Intracellular Ca^{2+} measurement

The intracellular Ca^{2+} concentration ($[Ca^{2+}]_i$) of cardiac fibroblasts was determined by the previously described method (10). Briefly, cells (1×10^5) were plated on glass-bottom, 35-mm dish and were loaded with 1 μM fura-2/AM in the cultured medium at 37°C for 30 min. The cells were washed with Tyrode solution containing 118 mM NaCl, 5.4 mM KCl, 2 mM $CaCl_2$, 2 mM $MgCl_2$, 10 mM Hepes (pH 7.4), 0.33 mM NaH_2PO_4, 10 mM glucose, and 30 mM taurine. Fluorescence images of GFP-positive cells were recorded and analyzed with a video image analysis system (Aquacosmos, Hamamatsu Photonics Co., Shizuoka). Resting $[Ca^{2+}]_i$ levels in CA-Gα_{13}-expressing cells were similar (60 – 90 nM) to GFP-expressing cells as analyzed by in vivo calibration.

Statistical analyses

The results are presented as the mean ± S.E.M. The data were accumulated under each condition from at least three independent experiments. For the measurement of $[Ca^{2+}]_i$, data of time course experiments were plotted from one of three similar experiments that were performed with more than 30 cells. The *P* values are the results of one way ANOVA followed by Bonferroni's *t*-test. In the ELISA assay, the *P* values are the results of Student's *t*-test.

Results

Activated Gα_{13} increases IL-1β and IL-6 mRNAs expression in cardiac fibroblasts

To examine whether G proteins are involved in cytokine production in cardiac fibroblasts, various CA mutants of Gα were expressed at 300 MOI. Among the various CA mutants, CA-Gα_{13} increased IL-1β mRNA expression by 6.3-fold and IL-6 mRNA expression by 15-fold, compared to LacZ-expressing cells (Fig. 1). The expression of CA-Gα_{12} did not increase IL-1β and IL-6 mRNAs. Although CA-Gα_q significantly increased IL-1β mRNA expression, the increase in IL-6 mRNA expression by CA-Gα_q was not significant. These results suggest that Gα_{13} predominantly regulates the induction of IL-1β and IL-6 mRNAs in cardiac fibroblasts.

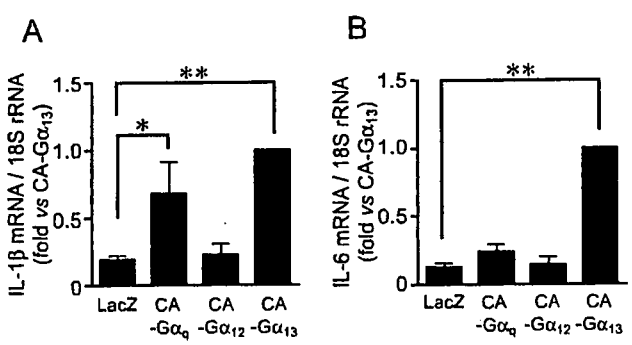

Fig. 1. Activated Gα_{13} increases IL-1β and IL-6 mRNAs expression in cardiac fibroblasts. Cells were infected with LacZ, CA-Gα_q, CA-Gα_{12}, or CA-Gα_{13} at 300 MOI, and IL-1β (A) and IL-6 (B) mRNAs expression were determined (n = 11). The fold increases were calculated by the values of CA-Gα_{13}-expressing cells set as 1. *P<0.05, **P<0.01 *vs* LacZ-expressing cells.

Involvement of NF-κB in activated Gα_{13}-induced cytokine mRNA induction

It has been reported that the promoter regions of IL-1β and IL-6 contain a putative NF-κB binding site (17, 18). Thus, we next examined whether NF-κB is involved in CA-Gα_{13}-induced expression of IL-1β and IL-6 mRNAs in cardiac fibroblasts. The induction of IL-1β and IL-6 mRNAs by CA-Gα_{13} was significantly suppressed by

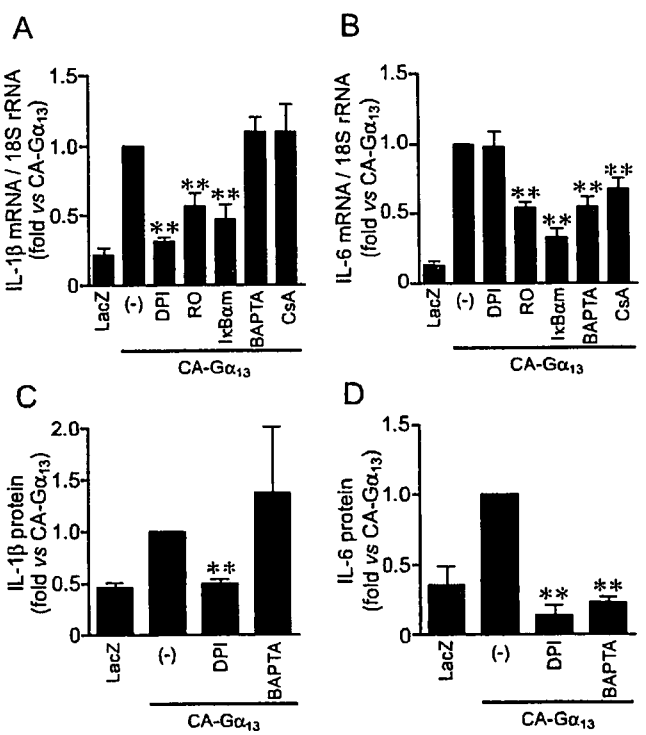

Fig. 2. Involvement of NF-κB, NFAT, ROS, or Ca^{2+} in the induction of IL-1β and IL-6 mRNAs and proteins by Gα_{13} activation. A, B: Cardiac fibroblasts were infected with LacZ and CA-Gα_{13} at 300 MOI or co-infected with CA-Gα_{13} at 300 MOI and IκBαm at 100 MOI. Three hours after infection, cells were treated for 33 h with 3 μM DPI, 4 μM Ro-106-9920 (RO), 3 μM BAPTA-AM (BAPTA), or 500 ng/ml cyclosporine A (CsA), and IL-1β (A) or IL-6 (B) mRNA expression were determined (n = 3 – 6). C, D: Three hours after infection of CA-Gα_{13} at 300 MOI, cells were treated for 33 h with 3 μM DPI or 3 μM BAPTA, and the concentration of IL-1β (C) or IL-6 (D) protein in cultured medium were determined by ELISA assay (n = 3). The fold increases were calculated by the values of CA-Gα_{13}-expressing cells set as 1. **P<0.01 *vs* CA-Gα_{13}-expressing cells.

treatment with 4 μM Ro-106-9920, a selective inhibitor of IκB phosphorylation, or by the expression of a non-phosphorylated form of IκBα (IkBam) at 100 MOI (Fig. 2). These results suggest that NF-κB regulates the induction of IL-1β and IL-6 mRNAs by CA-$G\alpha_{13}$.

Involvement of Ca^{2+} in the induction of IL-6 mRNA and protein by $G\alpha_{13}$ activation

Abbott et al. reported that NFAT functions as a cofactor of NF-κB signaling, leading to IL-6 mRNA induction by ATP receptor stimulation in vascular smooth muscle cells (11). We have previously demonstrated that the expression of CA-$G\alpha_{13}$ induces NFAT activation in cardiac fibroblasts (10). As NFAT activity is exclusively regulated by $[Ca^{2+}]_i$, we investigated the involvement of Ca^{2+} in CA-$G\alpha_{13}$-induced mRNA expression of IL-1β and IL-6. Treatment with 3 μM BAPTA-AM, an intracellular Ca^{2+} chelator, significantly suppressed IL-6 mRNA induction by CA-$G\alpha_{13}$, but not IL-1β mRNA induction (Fig. 2: A and B). In addition, the treatment with 500 ng/ml cyclosporine A, an inhibitor of calcineurin, also suppressed IL-6 mRNA induction by CA-$G\alpha_{13}$. However, cyclosporine A did not affect IL-1β mRNA induction by CA-$G\alpha_{13}$. As shown in Fig. 2, C and D, the expression of CA-$G\alpha_{13}$ increased the amounts of IL-1β in cultured medium by 2.2-fold (from 11.5 to 24.9 pg/ml) and IL-6 by 2.8-fold (from 8.7 to 24.7 pg/ml), compared to LacZ-expressing cells. Treatment with 3 μM BAPTA-AM completely suppressed the induction of IL-6 protein by CA-$G\alpha_{13}$, but not the induction of IL-1β protein. Furthermore, 3 μM BAPTA-AM significantly suppressed CA-$G\alpha_{13}$-induced NF-κB activation (Fig. 3). These results suggest that Ca^{2+}-dependent NFAT and NF-κB activation by $G\alpha_{13}$ activation mediates the induction of IL-6 mRNA and protein, but not IL-1β.

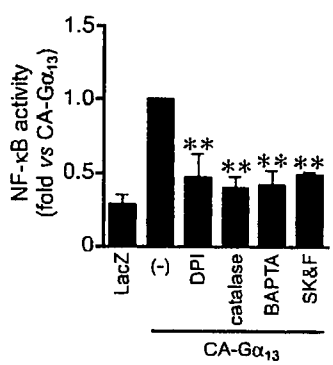

Fig. 3. Involvement of ROS and Ca^{2+} in NF-κB activation induced by $G\alpha_{13}$ activation. Cells were infected with LacZ and CA-$G\alpha_{13}$ at 100 MOI. Forty-two hours after infection, cells were treated for 6 h with 3 μM DPI, 100 U/ml catalase, 3 μM BAPTA-AM (BAPTA), or 30 μM SK&F96365 (SK&F) (n = 4 – 8). The fold increases were calculated by the values of CA-$G\alpha_{13}$-expressing cells set as 1. **$P<0.01$ *vs* CA-$G\alpha_{13}$-expressing cells.

Involvement of ROS in the induction of IL-1β and IL-6 by $G\alpha_{13}$ activation

A variety of evidence has suggested that ROS regulate NF-κB activity in mammalian cells (3). Thus, we next examined whether ROS participate in $G\alpha_{13}$-induced NF-κB activation and cytokine induction in cardiac fibroblasts. Treatment with 3 μM DPI, an inhibitor of NADPH oxidase, suppressed the induction of IL-1β mRNA and protein by CA-$G\alpha_{13}$ (Fig. 2: A and C). Although, the treatment with 3 μM DPI did not affect the CA-$G\alpha_{13}$-induced expression of IL-6 mRNA, DPI inhibited the increase in IL-6 protein by CA-$G\alpha_{13}$. Furthermore, the CA-$G\alpha_{13}$-induced NF-κB activation was also suppressed by 3 μM DPI or 100 U/ml catalase, an H_2O_2-degradating enzyme (Fig. 3). These results suggest that ROS mediate CA-$G\alpha_{13}$-induced increases in NF-κB activity and induction of IL-1β mRNA, IL-1β protein, and IL-6 protein.

Rho and Rho-kinase are not involved in IL-1β and IL-6 mRNAs induction by $G\alpha_{13}$ activation

It is generally thought that $G\alpha_{13}$-induced responses are exclusively mediated by small G protein Rho (19). However, the expression of C3 toxin at 100 MOI or treatment with 10 μM Y27632, a Rho-kinase inhibitor, did not affect the CA-$G\alpha_{13}$-induced increases in IL-1β and IL-6 mRNAs and NF-κB activation (Fig. 4). These results suggest that Rho and Rho-kinase do not participate in $G\alpha_{13}$-induced NF-κB activation and induction of IL-1β and IL-6 mRNAs.

Increased Ca^{2+} influx by $G\alpha_{13}$ activation

Our previous study has demonstrated that the expression of CA-Rho and CA-Rac promotes nuclear translocation of NFAT4 in cardiac fibroblasts (10). On the other hand, the present data indicate that $G\alpha_{13}$ induces NF-κB activation and IL-6 mRNA expression in a Ca^{2+}-dependent but Rho/Rho-kinase-independent mechanisms. As shown in Fig. 3, treatment with 30 μM SK&F96365, an inhibitor of receptor-activated non-selective cation channels (20), significantly suppressed NF-κB activation induced by CA-$G\alpha_{13}$. These results suggested that $G\alpha_{13}$ increases membrane Ca^{2+}-permeable channel activity that is not regulated by Rho and Rho-kinase. To examine whether $G\alpha_{13}$ regulates Ca^{2+} permeability in a Rho-independent manner, we determined the basal Ca^{2+} influx in CA-$G\alpha_{13}$-expressing cardiac fibroblasts. Under the basal conditions in normal Tyrode solution, $[Ca^{2+}]_i$ in CA-$G\alpha_{13}$-expressing cells was similar (about 60 – 90 nM) to that in green fluorescent protein

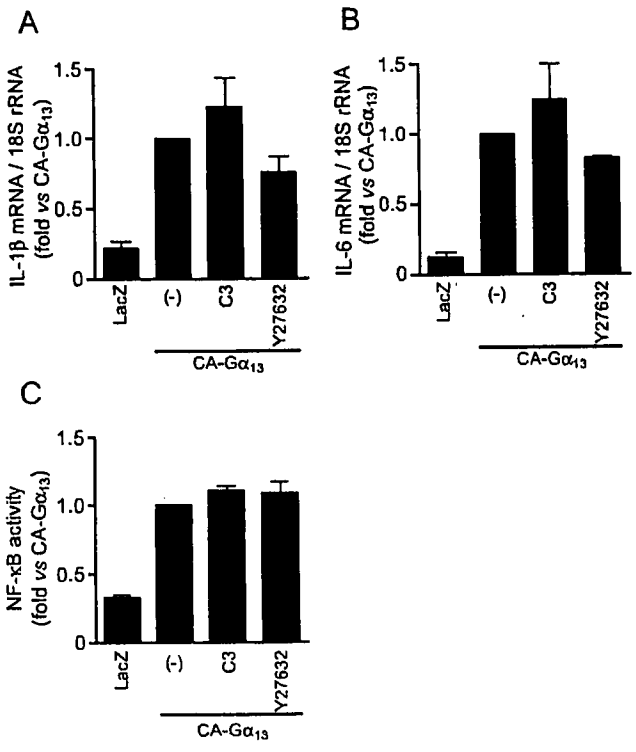

Fig. 4. Rho-and Rho-kinase-independent increases in IL-1β and IL-6 mRNAs induction by Gα_{13} activation. Cells were infected with LacZ and CA-Gα_{13} at 300 MOI or co-infected with CA-Gα_{13} at 300 MOI and C3 toxin at 100 MOI. Three hours after infection, cells were treated with 10 μM Y27632, and IL-1β (A) and IL-6 (B) mRNAs expression was determined (n = 4 – 5). C: Effects of C3 toxin and Y27632 on CA-Gα_{13}-induced NF-κB transcriptional activity were also determined. Forty-two hours after infection, cells were treated for 6 h with 10 μM Y27632, and NF-κB-dependent luciferase activity was determined (n = 4). The fold increases were calculated by the values of CA-Gα_{13}-expressing cells set as 1.

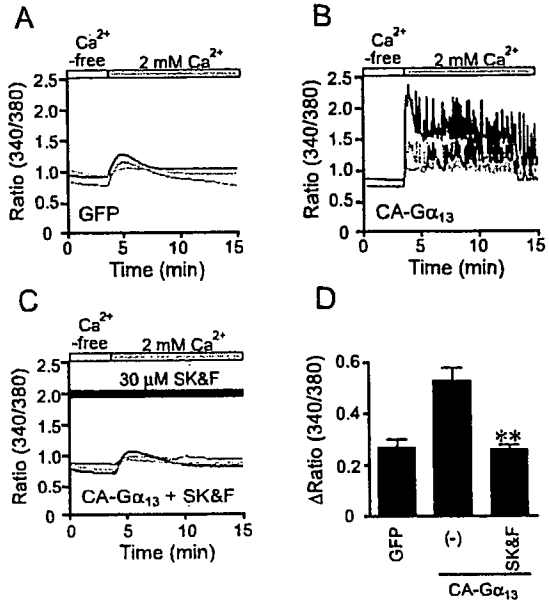

Fig. 5. Increases in basal Ca^{2+} influx induced by Gα_{13} activation. Four minutes after Ca^{2+} measurement in Ca^{2+}-free solution, basal Ca^{2+} influx was evaluated by the addition of 2 mM Ca^{2+}, and $[Ca^{2+}]_i$ was determined. SK&F96325 (SK&F, 30 μM) was treated for 10 min before the addition of extracellular Ca^{2+}. Representative time courses of Ca^{2+} responses in cardiac fibroblasts expressing GFP (A) or CA-Gα_{13} without (B) or with (C) SK&F are shown in the figure. D: The amplitude of maximum $[Ca^{2+}]_i$ rises (ΔRatio) induced by the addition of 2 mM extracellular Ca^{2+} was also calculated. $^{**}P<0.01$ *vs* CA-Gα_{13}-expressing cells.

(GFP)-expressing control cells. The resting $[Ca^{2+}]_i$ of CA-Gα_{13}-expressing cells was decreased by removal of extracellular Ca^{2+}, which was similar to the $[Ca^{2+}]_i$ level of control cells. The addition of 2 mM extracellular Ca^{2+} significantly increased $[Ca^{2+}]_i$ of CA-Gα_{13}-expressing cells (Fig. 5). This increase in $[Ca^{2+}]_i$ was completely suppressed by 30 μM SK&F96365. These results suggest that Ca^{2+} influx is constitutively increased in CA-Gα_{13}-expressing cells.

Discussion

In this study, we demonstrated that Gα_{13} activation increased the expression of IL-1β and IL-6 mRNAs and promotes the release of IL-1β and IL-6 proteins from cardiac fibroblasts (Figs. 1 and 2). It is generally thought that Gα_{12} and Gα_{13} share common signaling pathways to induce cellular responses (19). However, the induction of these cytokine mRNAs was rather specific for Gα_{13} (Fig. 1). We also found that the Gα_q signaling pathway was also involved in the expression of IL-1β mRNA in cardiac fibroblasts. Thus, our results suggest that both Gα_q and Gα_{13} regulate the expression of IL-1β mRNA, while only Gα_{13} regulates the expression of IL-6 mRNA in rat neonatal cardiac fibroblasts.

Our results also demonstrated that NF-κB was involved in the induction of both IL-1β and IL-6 mRNAs. The NF-κB activity was dependent on $[Ca^{2+}]_i$, as BAPTA-AM totally inhibited the activation (Fig. 3). However, the induction of IL-1β mRNA was not inhibited by BAPTA-AM, and the expression of IL-6 mRNA was partially inhibited by BAPTA-AM (Fig. 2: A and B). This apparent discrepancy may be explained by the several transcriptional factors involved in cytokine gene expression. The analysis of promoter regions of IL-1β and IL-6 genes shows that these regions contain several DNA binding sites for several transcriptional factors in addition to NF-κB, for instance AP-1, a ROS-sensitive transcriptional factor, and NFAT, a Ca^{2+}-sensitive transcriptional factor. These transcriptional factors synergistically regulate the transcription of cytokine mRNAs. We previously reported that CA-Gα_{13} increases NFAT and AP-1 transcriptional activities in

cardiac fibroblasts (10). Furthermore, the present results indicate that the induction of IL-1β mRNA by $G\alpha_{13}$ activation is mediated by ROS-dependent NF-κB activation, and that of IL-6 mRNA is mediated by Ca^{2+}-dependent NF-κB activation (Figs. 2 and 3). This implies that there are two kinds of NF-κB, which is functionally compartmentalized and respond separately to ROS or Ca^{2+}. We suggest that the expression of IL-1β mRNA induced by CA-$G\alpha_{13}$ requires a ROS-responsive NF-κB and AP-1 pathway, while IL-6 mRNA requires a Ca^{2+}-responsive NF-κB and NFAT pathway, even though both species of NF-κB synergistically regulate the NF-κB-dependent luciferase activity.

The amount of IL-1β released into culture medium was increased by CA-$G\alpha_{13}$, and this increase was inhibited by DPI (Fig. 2C). Thus, the inhibition of the expression of IL-1β protein by DPI was explained by the inhibition of mRNA induction. In contrast to IL-1β, the amount of IL-6 in culture medium but not the induction of IL-6 mRNA was inhibited by DPI (Fig. 2D). Therefore, DPI may inhibit the step(s) at translation and/or secretion of IL-6 protein.

As DPI suppressed $G\alpha_{13}$-induced IL-1β mRNA induction, $G\alpha_{13}$-induced ROS production may occur through NADPH oxidase activation. On the other hand, we have previously demonstrated that Rho and Rho-kinase mediate Rac-dependent NADPH oxidase activation upon Ang II receptor stimulation (10, 15). However, Rho and Rho-kinase did not participate in CA-$G\alpha_{13}$-induced NF-κB activity and cytokine mRNAs induction (Fig. 4). Thus, the Rho-independent pathway leading to NADPH oxidase activation may be activated by $G\alpha_{13}$ activation in cardiac fibroblasts.

In non-excitable cells, voltage-independent receptor-activated nonselective cation channels, including store-operated Ca^{2+} channels and transient receptor potential (TRP) channels, regulate basal Ca^{2+} influx (21). In fact, the CA-$G\alpha_{13}$-induced increases in $[Ca^{2+}]_i$ were completely suppressed by the treatment with SK&F96365. Thus, these results suggest that $G\alpha_{13}$-induced increase in Ca^{2+} influx is mediated by continuous activation of the nonselective cation channels in rat cardiac fibroblasts. This idea is in part supported by the previous report that stimulation of endothelin-1 receptor increased sustained Ca^{2+} influx through activation of G_{12} family G protein in rat arterial smooth muscle cells (20). We have previously reported that Rac1 is involved in JNK activation by regulating $[Ca^{2+}]_i$ in the H9c2 myoblast cell line (22). We have also demonstrated that $G\alpha_{13}$ activation by Ang II receptor stimulation increases Rac activity in cardiomyocytes (10, 15). However, the expression of CA-Rac1 did not affect IL-6 mRNA induction (data not shown). Therefore, another mechanism should be involved in $G\alpha_{13}$-induced activation of Ca^{2+} signaling. Further study is necessary for understanding the mechanism of sustained increase in the resting $[Ca^{2+}]_i$ induced by $G\alpha_{13}$ stimulation.

We also examined the effects of SK&F96365 on IL-1β and IL-6 mRNAs expression. However, the treatment of cells with SK&F96365 increased the basal expression of these cytokine mRNAs for yet unknown reasons (data not shown). Although SK&F96365 inhibited the further increases in these mRNAs expressions, the inhibition was partial. SK&F96365 also inhibited the increases in $[Ca^{2+}]_i$ and NF-κB activity. However, these inhibitions were not reflected by inhibition of mRNA expression. The expression of dominant negative forms of TRP channels or the suppression of TRP expression by RNAi may be necessary to demonstrate the involvement of TRP channels in IL-1β and IL-6 mRNAs expressions.

Several receptors are reported to couple to one or both members of the G_{12} family G proteins, based on direct or indirect methods of evaluating G protein activation (23). These receptors include angiotensin type 1 (AT1) receptor, endothelin-1 receptor, lysophosphatidic acid receptor, and 5-HT receptor. In the present study, we have demonstrated that $G\alpha_{13}$ activation increases the expression of IL-1β and IL-6 mRNAs and proteins in cardiac fibroblasts. As the stimulation of 5-HT_{2B} receptor or AT1 receptor has been reported to increase IL-1β or IL-6 production (5, 8), $G\alpha_{13}$ signaling pathways may participate in receptor-stimulated cytokine production in cardiac fibroblasts. We have not yet examined whether G_{13}-coupled receptor stimulation actually increases the expression of IL-1β and IL-6 mRNAs and proteins through the above pathways. Further studies will be necessary for the understanding of roles of $G\alpha_{13}$ signaling pathways in cytokine induction of cardiac fibroblasts.

A recent report has suggested that the strength of receptor signaling is centrally controlled through a cooperative loop between Ca^{2+} and an oxidant signal in B lymphocytes (24). We have previously demonstrated that both ROS and Ca^{2+} are required for $G_{12/13}$-mediated NFAT activation upon Ang II receptor stimulation in cardiac fibroblasts (10). Thus, ROS and Ca^{2+} generated by $G\alpha_{13}$ activation may cooperatively control the amplitude and duration of G_{13} protein-coupled receptor signaling in cardiac fibroblasts.

In conclusion, we have demonstrated a signal transduction pathway of $G\alpha_{13}$-induced increases in IL-1β and IL-6 mRNAs expression through NF-κB activation. NF-κB activation is regulated by both ROS and Ca^{2+}. However, these two signaling mediators distinctly regulate cytokine mRNA induction: ROS mediate IL-1β

mRNA induction and Ca^{2+} mediates IL-6 mRNA induction. The involvement of $G\alpha_{13}$ in cytokine mRNA induction in cardiac fibroblasts will provide a new insight into the cell-cell communication between cardiomyocytes and cardiac fibroblasts.

Acknowledgments

We thank Dr. Ryuji Inoue and Dr. Yushi Ito (Department of Pharmacology, Graduate School of Medical Sciences, Kyushu University) for the Aquacosmos imaging system, Dr. Hideki Sumimoto (Institute of Bioregulation, Kyushu University) for the luminometer, and Dr. Shigehiro Ohdo (Department of Medico-Pharmaceutical Sciences, Graduate School of Pharmaceutical Sciences, Kyushu University) for the Applied Biosystems 7500 Real-Time PCR System. We also thank Dr. Hiroyuki Tanaka (Department of Medical Plant Breeding, Graduate School of Pharmaceutical Sciences, Kyushu University) for help in the ELISA assay. This work was supported in part by a research grant (to M.N. and H.K.) from the Ministry of Education, Culture, Sports, Science, and Technology of Japan; in part by grants (to M.N.) from The Naito Foundation, The Uehara Foundation, The Kanae Foundation, The Suzuken Memorial Foundation, The Nakajima Memorial Foundation, Kao Foundation for Arts and Sciences, Takeda Science Foundation, and Japan Heart Foundation Research Grant; and a grant from Astellas Foundation for Research on Metabolic Disorders (to H. Kurose).

References

1 Brown RD, Ambler SK, Mitchell MD, Long CS. The cardiac fibroblast: therapeutic target in myocardial remodeling and failure. Annu Rev Pharmacol Toxicol. 2005;45:657–687.
2 Manabe I, Shindo T, Nagai R. Gene expression in fibroblasts and fibrosis: involvement in cardiac hypertrophy. Circ Res. 2002;91:1103–1113.
3 Siwik DA, Colucci WS. Regulation of matrix metalloproteinases by cytokines and reactive oxygen/nitrogen species in the myocardium. Heart Fail Rev. 2004;9:43–51.
4 Murray DR, Prabhu SD, Chandrasekar B. Chronic β-adrenergic stimulation induces myocardial proinflammatory cytokine expression. Circulation 2000;101:2338–2341.
5 Jaffre F, Callebert J, Sarre A, Etienne N, Nebigil CG, Launay JM, et al. Involvement of the serotonin 5-HT_{2B} receptor in cardiac hypertrophy linked to sympathetic stimulation: control of interleukin-6, interleukin-1beta, and tumor necrosis factor-alpha cytokine production by ventricular fibroblasts. Circulation. 2004;110:969–974.
6 Thaik CM, Calderone A, Takahashi N, Colucci WS. Interleukin-1β modulates the growth and phenotype of neonatal rat cardiac myocytes. J Clin Invest. 1995;96:1093–1099.
7 Fernandez L, Mosquera JA. Interleukin-1 increases fibronectin production by cultured rat cardiac fibroblasts. Pathobiology. 2002–2003;70:191–196.
8 Sano M, Fukuda K, Kodama H, Pan J, Saito M, Matsuzaki J, et al. Interleukin-6 family of cytokines mediate angiotensin II-induced cardiac hypertrophy in rodent cardiomyocytes. J Biol Chem. 2000;275:29717–29723.
9 Wollert KC, Drexler H. The role of interleukin-6 in the failing heart. Heart Fail Rev. 2001;6:95–103.
10 Fujii T, Onohara N, Maruyama Y, Tanabe S, Kobayashi H, Fukutomi M, et al. $G\alpha_{12/13}$-mediated production of reactive oxygen species is critical for angiotensin receptor-induced NFAT activation in cardiac fibroblasts. J Biol Chem. 2005;280:23041–23047.
11 Abbott KL, Loss II JR, Robida AM, Murphy TJ. Evidence that $G\alpha_q$-coupled receptor-induced interleukin-6 mRNA in vascular smooth muscle cells involves the nuclear factor of activated T cells. Mol Pharmacol. 2000;58:946–953.
12 Kurose H. $G\alpha_{12}$ and $G\alpha_{13}$ as key regulatory mediator in signal transduction. Life Sci. 2003;74:155–161.
13 Maruyama Y, Nishida M, Sugimoto Y, Tanabe S, Turner J H, Kozasa T, et al. $G\alpha_{12/13}$ mediates α_1-adrenergic receptor-induced cardiac hypertrophy. Circ Res. 2002;91:961–969.
14 Arai K, Maruyama Y, Nishida M, Tanabe S, Takagahara S, Kozasa T, et al. Differential requirement of $G\alpha_{12}$, $G\alpha_{13}$, $G\alpha_q$, and $G\beta\gamma$ for endothelin-1-induced c-Jun NH_2-terminal kinase and extracellular signal-regulated kinase activation. Mol Pharmacol. 2003;63:478–488.
15 Nishida M, Tanabe S, Maruyama Y, Mangmool S, Urayama K, Nagamatsu Y, et al. $G\alpha_{12/13}$- and reactive oxygen species-dependent activation of c-Jun NH_2-terminal kinase and p38 mitogen-activated protein kinase by angiotensin receptor stimulation in rat neonatal cardiomyocytes. J Biol Chem. 2005;280:18434–18441.
16 Nishida M, Maruyama Y, Tanaka R, Kontani K, Nagao T, Kurose H. $G\alpha_i$ and $G\alpha_o$ are target proteins of reactive oxygen species. Nature. 2000;408:492–495.
17 Monks BG, Martell BA, Buras JA, Fenton MJ. An upstream protein interacts with a distinct protein that binds to the cap site of the human interleukin 1β gene. Mol Immunol. 1994;31:139–151.
18 Kaiser P, Rothwell L, Goodchild M, Bumstead N. The chicken proinflammatory cytokines interleukin-1β and interleukin-6: differences in gene structure and genetic location compared with their mammalian orthologues. Anim Genet. 2004;35:169–175.
19 Wettschureck N, Offermanns S. Mammalian G proteins and their cell type specific functions. Physiol Rev. 2005;85:1159–1204.
20 Kawanabe Y, Okamoto Y, Miwa S, Hashimoto N, Masaki T. Molecular mechanisms for the activation of voltage-independent Ca^{2+} channels by endothelin-1 in chinese hamster ovary cells stably expressing human $endothelin_A$ receptors. Mol Pharmacol. 2002;62:75–80.
21 Clapham DE. TRP channels as cellular sensors. Nature. 2003;426:517–524.
22 Nishida M, Nagao T, Kurose H. Activation of Rac1 increases c-Jun NH_2-terminal kinase activity and DNA fragmentation in a calcium-dependent manner in rat myoblast cell line H9c2. Biochem Biophys Res Commun. 1999;262:350–354.
23 Riobo NA, Manning DR. Receptors coupled to heterotrimeric G proteins of the G_{12} family. Trends Pharmacol Sci. 2005;26:146–154.
24 Singh DK, Kumar D, Siddiqui Z, Basu SK, Kumar V, Rao KV. The strength of receptor signaling is centrally controlled through a cooperative loop between Ca^{2+} and an oxidant signal. Cell. 2005;121:281–293.

nature
chemical biology

Nitric oxide activates TRP channels by cysteine S-nitrosylation

Takashi Yoshida[1–3], Ryuji Inoue[4], Takashi Morii[5], Nobuaki Takahashi[1], Shinichiro Yamamoto[1], Yuji Hara[1], Makoto Tominaga[2,3], Shunichi Shimizu[6], Yoji Sato[7] & Yasuo Mori[1]

Transient receptor potential (TRP) proteins form plasma-membrane cation channels that act as sensors for diverse cellular stimuli. Here, we report a novel activation mechanism mediated by cysteine S-nitrosylation in TRP channels. Recombinant TRPC1, TRPC4, TRPC5, TRPV1, TRPV3 and TRPV4 of the TRPC and TRPV families, which are commonly classified as receptor-activated channels and thermosensor channels, induce entry of Ca^{2+} into cells in response to nitric oxide (NO). Labeling and functional assays using cysteine mutants, together with membrane sidedness in activating reactive disulfides, show that cytoplasmically accessible Cys553 and nearby Cys558 are nitrosylation sites mediating NO sensitivity in TRPC5. The responsive TRP proteins have conserved cysteines on the same N-terminal side of the pore region. Notably, nitrosylation of native TRPC5 upon G protein–coupled ATP receptor stimulation elicits entry of Ca^{2+} into endothelial cells. These findings reveal the structural motif for the NO-sensitive activation gate in TRP channels and indicate that NO sensors are a new functional category of cellular receptors extending over different TRP families.

Ionized calcium (Ca^{2+}) is the most common signal-transduction molecule in cells ranging from bacteria to brain neurons[1]. Ca^{2+} is derived from two sources: from outside of cells, Ca^{2+} enters by passing through Ca^{2+}-permeable channels in the plasma membrane; from the inside of cells, it can be released from the endoplasmic reticulum (ER) through channels embedded in internal membrane networks. Groups of plasma membrane channels that are permeable to Ca^{2+} (or cations in general) act as sensors by translating cellular stimuli into electrical signals—namely membrane potential changes—or chemical signals such as changes in intracellular Ca^{2+} concentration ($([Ca^{2+}]_i)$[2–4]. *Drosophila melanogaster* TRP protein and its homologs are putative six-transmembrane polypeptide subunits that assemble into tetramers to form channels. In mammalian systems, TRP channels comprise six related protein subfamilies: TRPC, TRPV, TRPM, TRPA, TRPP and TRPML (ref. 5).

TRP channels are activated by diverse stimuli, including receptor stimulation, heat, osmotic pressure, and mechanical and oxidative stress from the extracellular environment and from inside the cell[3,4]. The TRPC homologs are receptor-activated Ca^{2+}-permeable cation channels (RACCs) that are activated upon receptor stimulation that induces phospholipase C (PLC) to hydrolyze phosphatidylinositol-4,5-biphosphate (PIP_2) into inositol-1,4,5-trisphosphate (IP_3) and diacylglycerol[6,7]. RACCs include store-operated channels (SOCs) activated by IP_3-induced Ca^{2+} release and depletion of ER Ca^{2+} stores. Among seven TRPC homologs (TRPC1, TRPC2, TRPC3, TRPC4, TRPC5, TRPC6 andTRPC7), TRPC1, TRPC3 and TRPC4 form SOCs, whereas TRPC5, TRPC6, TRPC7 and some TRPC3 channels are distinguishable from SOCs. In contrast to TRPCs, TRPV Ca^{2+}-permeable channels can be functionally defined as thermosensors [3,5,8,9]. TRPV1, which was originally identified as the receptor for the vanilloid compound capsaicin, is responsive to heat (>43 °C), to proton concentration (pH < 5.6), to the intrinsic ligand anandamide and to PLC-linked receptor stimulation[5]. High temperature also activates TRPV2 (>52 °C), TRPV3 (>31 °C or >39 °C) and TRPV4 (>27 °C). TRPV5 and TRPV6 comprise a different subfamily because they are activated by $[Ca^{2+}]_i$ (refs. 3,5). Thus, characteristic activation triggers functionally distinguish sensor cation channels formed by molecularly distinct TRPC- and TRPV-family proteins.

NO is another pleiotropic cell signaling molecule that controls diverse biological processes[10,11]. According to the classical view, cyclic GMP is the mediator of NO signaling. However, the importance of a cGMP-independent pathway through protein S-nitrosylation is increasingly recognized by researchers in the field of NO signal transduction[10,11]. Because nitrosothiols are exceptionally labile owing to their reactivity with intracellular reducing reagents such as ascorbic acid, S-nitrosylation functions as a reversible post-translational modification analogous to phosphorylation. Cysteine modifications of proteins are also elicited by other NO-related species, reactive oxygen species, glutathione disulfide and free sulfhydryl-specific reactive disulfide[11,12]. However, these modifications are rather

[1]Department of Synthetic Chemistry and Biological Chemistry, Graduate School of Engineering, Kyoto University, Kyoto 615-8510, Japan. [2]Center for Integrative Bioscience, National Institute for Physiological Sciences, Okazaki, Aichi 444-8585, Japan. [3]School of Life Science, The Graduate University for Advanced Studies, Okazaki, Aichi 444-8585, Japan. [4]Department of Physiology, Fukuoka University, Fukuoka 814-0180, Japan. [5]Institute of Advanced Energy, Kyoto University, Uji, Kyoto 611-0011, Japan. [6]Department of Pathophysiology, School of Pharmaceutical Sciences, Showa University, Tokyo 142-8555, Japan. [7]Division of Cellular and Gene Therapy Products, National Institute of Health Sciences, Tokyo 158-8510, Japan. Correspondence should be addressed to Y.M. (mori@sbchem.kyoto-u.ac.jp).

Received 20 March; accepted 4 August; published online 24 September 2006; doi:10.1038/nchembio821

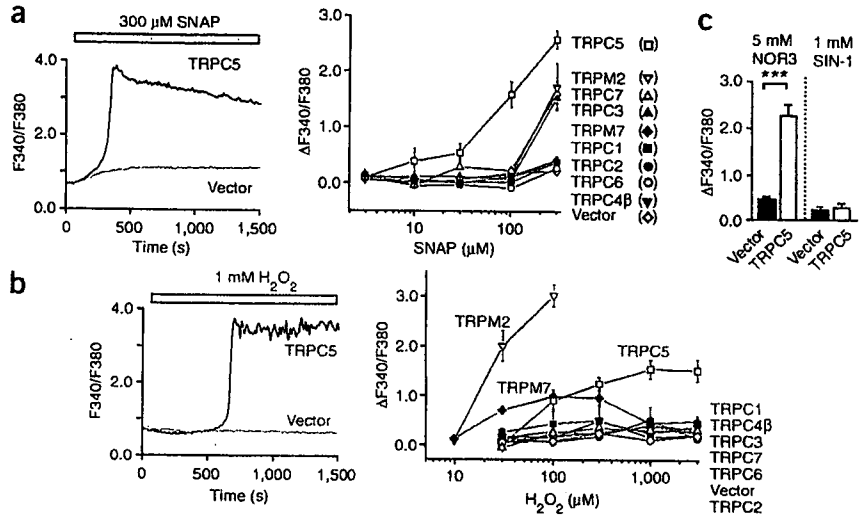

Figure 1 NO activates TRPC5-mediated Ca^{2+} response. (a,b) $[Ca^{2+}]_i$ rises (340:380-nm fluorescence ratio; F340/F380) evoked by SNAP (a) and H_2O_2 (b) applied during periods indicated by shaded bars in the presence of 2 mM extracellular Ca^{2+}. Representative time courses (left) and dose-response relationships of maximal $[Ca^{2+}]_i$ rises (ΔF340/F380) (right) in HEK cells transfected with TRP homologs or vector (n = 6–61). Data points are mean ± s.e.m. (c) Maximal $[Ca^{2+}]_i$ rises induced by NOR3 and SIN-1 (n = 19–31). ***$P < 0.001$.

pathophysiological, although they can be viewed as existing on a continuum that relates concentrations of reactive species to the form and consequences of modification. Thus, S-nitrosylation alone conveys physiological redox-based cellular signals[11].

Ca^{2+} and NO signals are precisely coordinated with each other. Among three distinct isoforms of NO synthases (NOSs) responsible for NO production, $[Ca^{2+}]_i$ elevation is essential for activation of Ca^{2+}-dependent endothelial NOS (eNOS) and neuronal NOS (nNOS)[13]. Furthermore, IP_3-induced Ca^{2+} release and RACC-mediated Ca^{2+} influx via PLC activation is efficiently evoked upon receptor stimulation by physiological agonists such as vasodilators, thereby leading to eNOS activation in endothelial cells and other cell types[14–16]. However, it is still unclear whether activation of eNOS requires specific modes of upstream Ca^{2+}-mobilizing mechanism or RACC subtypes formed by particular TRPCs (refs. 16–20), whereas NMDA (*N*-methyl-D-aspartate) receptors in neurons and L-type voltage-dependent Ca^{2+} channels in muscles are known to conduct nNOS-activating Ca^{2+} influx[21]. Feedback regulation of Ca^{2+} signaling by NO remains even more elusive[22]: both positive[23–25] and negative[26,27] regulation by NO of Ca^{2+} mobilization pathways including RACCs has been reported. Physiological protein targets for cysteine S-nitrosylation include postsynaptic NMDA receptors and skeletal-muscle ryanodine-receptor Ca^{2+} release channels[11]. However, these channels involved in Ca^{2+} signaling are very restricted in tissue distribution and have specific physiological functions, compared with the widely recognized generality of NO signaling via protein S-nitrosylation, Ca^{2+} signaling, and their cross talk. Therefore, to understand more general molecular mechanisms that link the two key signals, S-nitrosylation targets must be identified among more ubiquitous Ca^{2+}-mobilizing ion channels. This would ultimately provide insights into the activation gating that underlies sensor function in TRP channels.

Here, we describe cysteine modification as a previously unknown mechanism that triggers activation gating of TRP channels. Chemical labeling assays using TRPC5 mutants reveal modification of Cys553 and Cys558 (whose counterparts are harbored by the NO-responsive TRPC and TRPV members) on the N-terminal side of the pore-forming region. Further studies using cultured endothelial cells, in combination with the previously reported wide distribution of the NO-responsive TRPC and TRPV channels among diverse tissues[5],

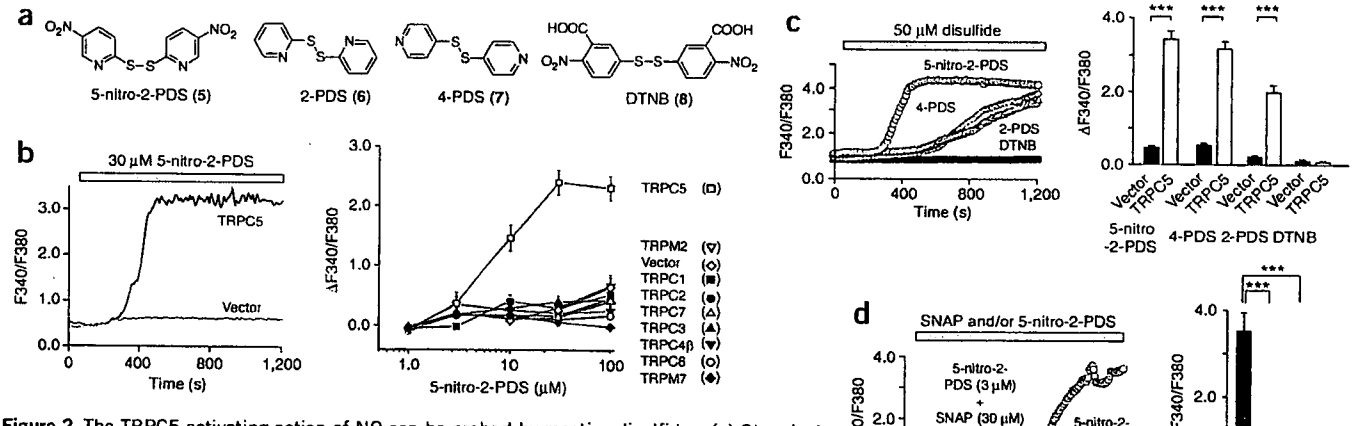

Figure 2 The TRPC5-activating action of NO can be probed by reactive disulfides. (a) Chemical structures of reactive disulfides. (b) TRPC5-mediated Ca^{2+} responses to 5-nitro-2-PDS: representative time courses (left) and dose-response relationships (right). (c) TRPC5 responses to various reactive disulfides (50 μM; n = 9–23): averaged time courses (left) and maximal $[Ca^{2+}]_i$ rises (right). ***$P < 0.001$. (d) 30 μM SNAP and 3 μM 5-nitro-2-PDS induce only marginal Ca^{2+} responses by individual applications (n = 25 and n = 26, respectively), but in combination they trigger robust TRPC5-mediated Ca^{2+} responses (n = 18): averaged time courses (left) and maximal $[Ca^{2+}]_i$ rises (right). Data points are mean ± s.e.m. ***$P < 0.001$.